J. Fluid Mech. (1985), *vol.* 155, *pp.* 141–174
Printed in Great Britain

Sinusoidal flow relative to circular cylinders

By C. H. K. WILLIAMSON
Engineering Department, University of Cambridge

(Received 30 May 1984 and in revised form 14 December 1984)

The motions of vortices around single cylinders and around pairs of cylinders in relative sinusoidal flow are investigated in this paper. Using simultaneous flow visualization and force measurements, the vortex motions are related to the fluid-induced lift and in-line forces. For the single cylinder, several repeatable patterns of vortex shedding are identified within particular ranges of flow amplitude. The process of pairing of vortices from a previous half cycle with those in a present half cycle is fundamental to all the patterns. Visualization is shown to be more effective in a reference frame which is fixed with respect to the undisturbed fluid rather than with respect to the cylinders. For this reason, the examples of vortex motions are taken from a rig in which vertical cylinders are oscillated in a tank of fluid. By oscillating a pair of cylinders over a range of gaps, orientations and amplitudes, it is found that the vortex-shedding patterns identified for a single cylinder can synchronize either in phase or in antiphase between the two cylinders. Such observations help to explain how lift and in-line forces are influenced by cylinder proximity and in some cases these forces are significantly magnified. Force coefficients are evaluated for both the single cylinder and the pair of cylinders.

1. Introduction

There are fundamental differences between the vortex motions and induced forces on a cylinder in oscillatory flow as compared with one in a steady stream. In oscillatory flow the fluid reverses direction, causing the vortex wake of one half cycle to sweep past the body during a subsequent half cycle. This flow reversal has a major effect on the magnitudes of the fluid-induced forces, and also on the fundamental frequency of the lift force.

The study of two-dimensional oscillatory flows is of importance to the case of wave-induced forces on cylindrical structures, in that it is a first step to understanding the complex three-dimensional wave–structure interaction. In particular, wake reversal is a feature of both the two-dimensional and wave problem, and the vortex motion identified in low-Reynolds-number two-dimensional flow should be representative of some of the vortex motions found around cylinders in waves. The main application for a study of the hydrodynamic interference between a pair of cylinders is to the case of forces on neighbouring cylindrical members of offshore structures. One example could be the groups of cylindrical riser tubes which transport oil from the seabed to the surface. For example, when the cylinder pair of the present study has a spacing often found in riser groups (5 diameters between axes), significant flow interference takes place. However, the present idealized study can only be suggestive of possible flow characteristics around full-scale structures.

In practice, the prediction of fluid-induced drag forces in oscillatory or wave flow

is based on an equation due to Morison *et al.* (1950). They proposed a representation for the in-line force per unit length as

$$F = \tfrac{1}{2}\rho D C_D U|U| + \tfrac{1}{4}\pi\rho D^2 C_m \dot{U} \tag{1}$$

for a circular cylinder, where ρ is the fluid density, D is the body diameter and U is the fluid velocity. The coefficients C_D and C_m have been evaluated experimentally from full-scale and laboratory studies in a large number of investigations.

Keulegan & Carpenter (1958) placed a vertical cylinder beneath a standing wave in a wave tank, and found the average values of C_m and C_D to be functions of Keulegan–Carpenter number (Kc) where $Kc = U_m T/D$ (U_m = maximum fluid velocity, T = period). In sinusoidal flow, $Kc = 2\pi A/D$; thus Kc is proportional to the flow amplitude A.

The use of U-tubes to generate closely unidirectional sinusoidal flow past bodies has clarified some of the important parameters affecting the fluid-induced forces. Using a U-tube, Sarpkaya (1976) has found that C_m and C_D depend not only on Kc, but also on a parameter β which is proportional to Reynolds number Re; $\beta = Re/Kc = D^2 T\nu$, where ν is the kinematic viscosity.

Maull & Milliner (1978) have pointed out the possible usefulness of a Blasius force expression for the lift and in-line force, comprising an unsteady irrotational term and a term due to the strength and motion of the large rolled-up vortices in the wake. The Blasius equation is strictly only applicable in inviscid flow but may be used in an approximate manner to relate the induced forces with the main shed vortex motions. Graham (1980) has used the Blasius equation in a discrete-vortex model of a cylinder in sinusoidal flow and represented the clouds of vorticity by large numbers of small point vortices. He wrote the force equation (with Y and X as lift and in-line force) as

$$X + \mathrm{i}Y = \tfrac{1}{4}\pi\rho D^2 C_m \dot{U} - \mathrm{i}\rho \Sigma \frac{\partial}{\partial t}(\Gamma_n Z_n). \tag{2}$$

The sum is taken over all the vortex circulations Γ_n at positions Z_n and at their corresponding image positions in the cylinder, and C_m is the 'inertia' coefficient for irrotational flow. (C_m has a potential value of 2.0 for a circular cylinder in an accelerating fluid).

The use of visualization has increased understanding of the significance of vortices in fluid loading. Bearman, Graham & Singh (1979), using a U-tube, report the observation of some near-repeatable vortex patterns. The main vortex patterns above $Kc \approx 8$ were found to be a 'sideways' street (for $8 < Kc < 15$) and a cyclic regime (for $15 < Kc < 25$). Above $Kc \approx 25$, they found that the wake resembled a limited-length Kármán street in each half cycle. In the sideways street each successive main vortex shed per half cycle moved away from the cylinder on one side only (at around 90° to the oscillatory flow direction). The cyclic wake is one where a vortex pair convects away from the cylinder at 30°/40° to the flow direction in each half cycle. Successive pairs move away from opposite quadrants of the cylinder and in opposite directions.

The case of cylinder groups in oscillatory flow is a problem far less studied than the isolated-cylinder case. It is possible for the flow and forces to be significantly modified due to hydrodynamic interference effects. Zdravkovich (1977) has reviewed some of these effects between pairs of cylinders in steady flow. For oscillatory flow, the main thrust of previous work on cylinder groups has been in the measurement of forces on groups of cylinders.

Laird & Warren (1963) measured the total lift and in-line force on a 24-cylinder

bundle in sinusoidal flow at a large amplitude corresponding to $Kc = 165$. They found that the fluctuating total lift could be as large as the total drag. They thus suggested that a certain amount of lift-force synchronization may be present throughout the cylinder bundle.

Bushnell (1977) investigated the maximum forces on one cylinder in a 3×3 square array of cylinders and in pairs of cylinders in the sinusoidal flow of a pulsating water tunnel. Orientations of these arrays were varied at 0°, 20° and 40° between the flow direction and the line joining the cylinder centres. He conducted his experiments over large amplitudes corresponding with $Kc > 30$, and kept his cylinder spacing constant at $g^* = 2.0$ (where g^* = gap between cylinder surfaces/diameter). He found that the shielding effect of an upstream cylinder on a downstream cylinder produced a decrease of the in-line force but a significant increase in the lift, which was greatest at 20°. Bushnell stated that the similarity in the results between the two-cylinder array and the 3×3 array implied that no new features are likely in larger arrays.

Sarpkaya (1980) arranged a pair of cylinders in a U-tube at orientations of 0°, 30°, 60° and 90°, and measured C_m and C_D as well as lift-force coefficients C_L. The gaps were varied as $g^* = 0.5$, 1.5 and 2.5 over a range of flow amplitudes corresponding with $Kc = 10$ to 100. He found a similar shielding effect and increase of lift for a downstream cylinder as found by Bushnell for the 30° orientation (when $g^* < 1.5$), but only for $Kc > 40$. Below this amplitude the lift was diminished compared with the isolated-cylinder case. He also found no increase in the lift forces at 60° or 90° as the gaps were reduced, even at the smallest spacing. Sarpkaya concluded that the cylinder forces gradually approach their isolated-cylinder values as the flow amplitude becomes comparable to or smaller than the cylinder spacings.

Chakrabarti (1981, 1982) measured the lift and in-line force for one cylinder out of a 2, 3 or 5 cylinder row arranged side-by-side to oncoming waves in a tank. As he reduced the cylinder gaps the in-line force increased and, for the outer cylinder positions, the maximum lift coefficient is largest and increases above the isolated-cylinder value for very small spacings of $g^* = 0.33$.

In the above studies of cylinder groups in oscillatory flow it seems that no flow visualization has been undertaken and also no comparison has been made of simultaneous force measurements on two or more cylinders. Both of these features provide the basis of the present investigation concerning the cylinder pair, and reveal the existence of synchronization of the vortex shedding between cylinders. This characteristic of flow interference can lead to a synchronization of the lift-force fluctuations across the cylinder pair and has hitherto not been investigated.

The present study of the vortex motions and fluid forces on cylinders comprises simultaneous flow visualization and force measurements using an oscillating-cylinder tank. Force coefficients are evaluated for the single cylinder from a large U-tube and coefficients for the cylinder pair from the tank. The flow past a body in incompressible fluid of constant density is kinematically the same regardless of whether the body accelerates through the fluid or the fluid accelerates past the body (see for example Lighthill 1979). The only difference lies in a buoyancy-like force in-line with the flow caused by the pressure gradient within the fluid, when the fluid is accelerating past the body. The pressure gradient force increases the value of C_m in (1) by 1.0 when the fluid accelerates compared with that value of C_m when it is the body accelerating. It is expected from the above that the flow patterns in the two reference frames will be the same.

The flow visualization using surface particles in the tank, when the reference frame is fixed with respect to the undisturbed fluid, is markedly clearer than visualization

initially carried out using neutrally buoyant polystyrene beads in the U-tube. Using such a frame of reference in the tank, the vortex motions are not masked by a superposed free stream. Typical visualization possible with both frames of reference are compared in §3.

Simultaneous flow visualization and force measurements enable us to relate the shapes of the force profiles for the single cylinder (in particular the lift force) directly to the observed vortex motions. In §3.1, for each flow regime, schematic diagrams of typical force profiles are related to corresponding vortex motions. For the pair of cylinders in §3.2, the existence of vortex-shedding synchronization mentioned earlier, is found for certain cylinder geometries. Where the lift is in-phase across a cylinder group we can expect a large total lift on the cylinder bundle which may be comparable in magnitude to the drag force, and at a higher frequency. Where the lift is in antiphase between neighbouring cylinders it may be important to consider possible lateral vibrations of the cylinders. The orientations of the cylinders in §3.2 are 0°, 45° and 90°, for cylinder spacings of $0 < g^* < 4.0$, and flow amplitudes corresponding with $0 < Kc < 55$. The lift and in-line forces on both cylinders are recorded at the same time, which enables a link to be made between the synchronized vortex patterns and the cylinder forces.

Root mean square lift and in-line force coefficients are measured in §4 for both the single cylinder using the U-tube and for the cylinder pair using the tank. The r.m.s. in-line force coefficient is chosen to quantify force, rather than the 'Morison' coefficients in (1), because for the cylinder pair it indicates more clearly how the total force is modified as pair geometry is varied. Some of the trends in the force measurements of §4 are explained with reference to the flow patterns described in §3.

2. Experimental methods

The U-tube used for some of the force measurements (and originally for flow visualization) for the single cylinder is constructed of aluminium and perspex. The upright limbs are of height 2.65 m and the base is of length 3.73 m. The cross-section of the vertical limbs and horizontal section of the U-tube is 0.45 m × 0.48 m. The test cylinder of 0.05 m diameter is suspended at each end by arm supports in the right-hand limb of the U-tube. The cylinder is connected to the supports only via a thin 0.005 m tube, upon which strain gauges are mounted for force measurement. Water height is measured by a capacitance-wire system situated in the right-hand limb of the U-tube. The water is forced to oscillate in the U-tube at the resonant frequency by an oscillating horizontal plate in the left-hand limb. The range of Kc attainable with this rig is $0 < Kc < 35$, and the value of β is 730. The root-mean-square lift and in-line force coefficients are calculated from force measurements stored on a tape recorder and averaged over 40 cycles on a Cambridge Electronic Design 'Alpha' computer.

The oscillating-cylinder rig in which vertical cylinders are horizontally oscillated, has internal dimensions 2.4 m long and 0.9 m deep by 0.73 m wide, and is shown schematically in figure 1. The gap between the bottom tip of the vertical cylinders and the false floor is 0.2 cm. The cylinders are attached at their upper ends to a horizontal perspex plate which is secured to an oscillating framework sliding on bearings along horizontal tracks at the sides of the tank. The frame is oscillated by means of a wire system around pulleys (tensioned by weights) shown in figure 1, and one end of the tensioned wire system is attached eccentrically to a motor flywheel. Strain gauges are attached to the surface of the cylinder between the perspex plate

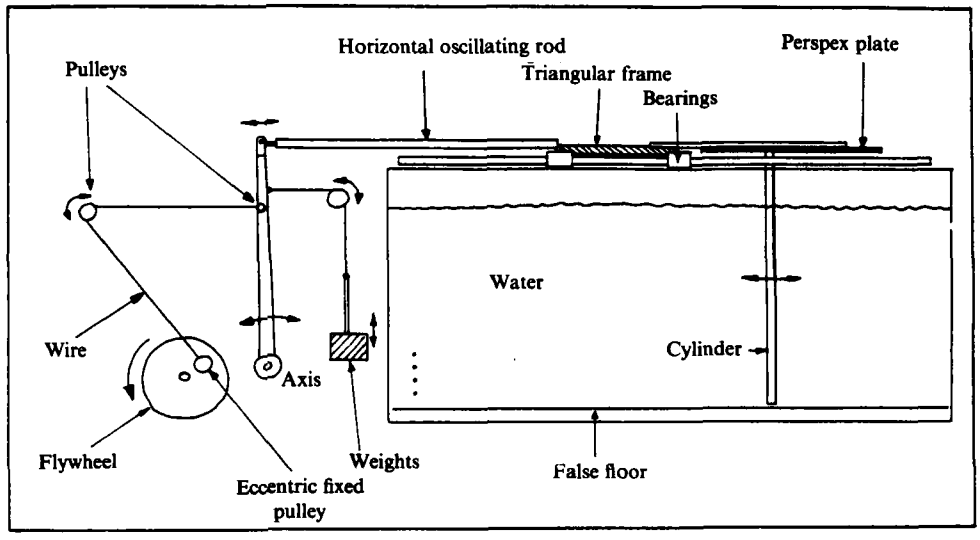

FIGURE 1. Schematic side view of the experimental rig to oscillate vertical cylinders in a tank of fluid.

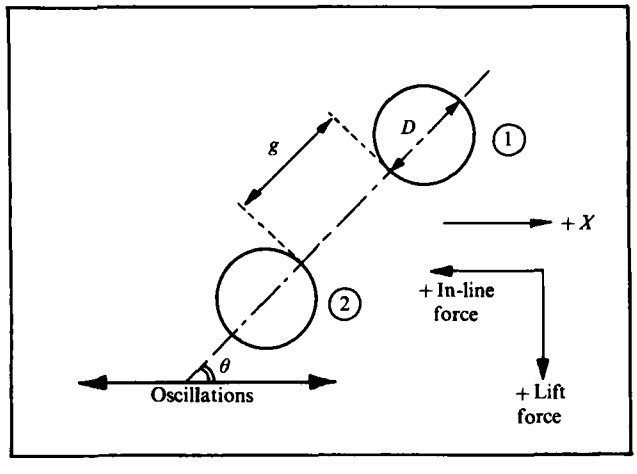

FIGURE 2. Geometry of the cylinder pair. Cylinder gaps are defined by g^*, where $g^* = g/D$. Orientations are defined by θ, where θ is the angle between the oscillation direction and the line joining cylinder centres. Positive lift and in-line force directions for cylinders 1 and 2 are shown.

and the water surface, for force measurements. The cylinders are of length 0.7 m with diameter of 0.012, 0.025 and 0.05 m, although strain gauges were only used on the 0.025 m cylinder giving a β value of 255. Oscillation amplitudes corresponding to $Kc < 60$ are used for visualization, and $Kc < 35$ for the force measurements. Displacement is measured with a linear transducer, and its signal along with the force signals are passed simultaneously into an ultraviolet Recorder and Tape Recorder. Analysis for the cylinder pair comprised the conditional partitioning of the digitized force signals into upstream and downstream half cycles. For each half cycle, force coefficients are found averaged from 40 half cycles for each geometry and amplitude. The inertia force of the cylinders themselves is subtracted from the measured in-line

forces. The diagram in figure 2 shows how the geometry of the cylinder pair is defined. In the force diagrams of §3.2, positive lift, in-line force and displacement on each cylinder (1) and (2) are defined as shown in figure 2. By photographing with a Nikon motordrive camera vertically downwards from above the horizontal perspex plate an unobstructed view around the cylinders is obtained. The surface of the water is sprinkled with aluminium powder and light sources comprise two slide projectors of 250 W each and 1000 W Halogen bulb placed around the tank edges. The camera may be fixed with respect to the cylinder or fixed with respect to the undisturbed fluid. The force measurements from both the U-tube and the tank have not been corrected for blockage or end effects.

3. Flow visualization and force measurements

3.1. *Vortex flow regimes for a single cylinder*

When an isolated cylinder is subjected to relative oscillatory flow certain repeatable vortex-shedding patterns are found to occur within particular ranges of flow amplitude. Each of these patterns reflects the shedding of a particular number of vortices per half cycle. A rough guide to the ranges of flow amplitude or Kc corresponding to each of the flow regimes which will be described in this section, is given in figure 3(*a*). Each wake pattern may continue in bursts of large numbers of cycles, but can intermittently change from one mode to another. For example, a wake which convects predominantly to one side of the cylinder (at large angles to the oscillation direction) can intermittently swap sides. Almost regular lift-force oscillations may be induced by these particular vortex wakes, and typical examples are shown in figure 3(*b*), with their corresponding water-displacement trace shown below them. Each of these four force traces are indications of specific vortex patterns named in figure 3(*a*) and are described below.

The relation of the vortex motions to the lift-force profiles in each regime has been found by simultaneous photography of the vortices with measurements of cylinder forces. In fact, every time a still photograph (or a ciné frame) was exposed, an electrical circuit was closed which resulted in a small d.c. 'jump' on an output trace upon which the forces were also recorded. The vortex growth and motions that are mainly responsible for certain force fluctuations were then identified with reference to the Blasius equation (2). Each schematic force profile and its corresponding description of vortex motions in the present paper is based upon such detailed simultaneous measurements in Williamson (1982). The force traces in this section are qualitative in that it is their shape which reflects the corresponding vortex motions. The quantitative measurements in the form of coefficients are included in §4.

Below $Kc = 7$, there are no major vortices shed during a half cycle although pairs of small vortices are formed each time the flow reverses. Large vortices are shed in each half cycle when $Kc > 7$. The transverse-street and double-pair patterns described and visualized in the present paper correspond with the reported observations of a sideways street and a cyclic regime in Bearman, Graham & Singh (1979). These patterns represent one and two vortices respectively, shed in each half cycle. In the present paper, the system of vortex pairing present in the above wake patterns is also a feature of a greater number of patterns, including those found at higher amplitudes and involving more vortices shed per cycle.

In the flow-visualization photographs the arrows indicate the direction of cylinder travel along with the approximate position of the cylinder between its extreme excursions. The arrows in the schematic diagrams of flow patterns also indicate

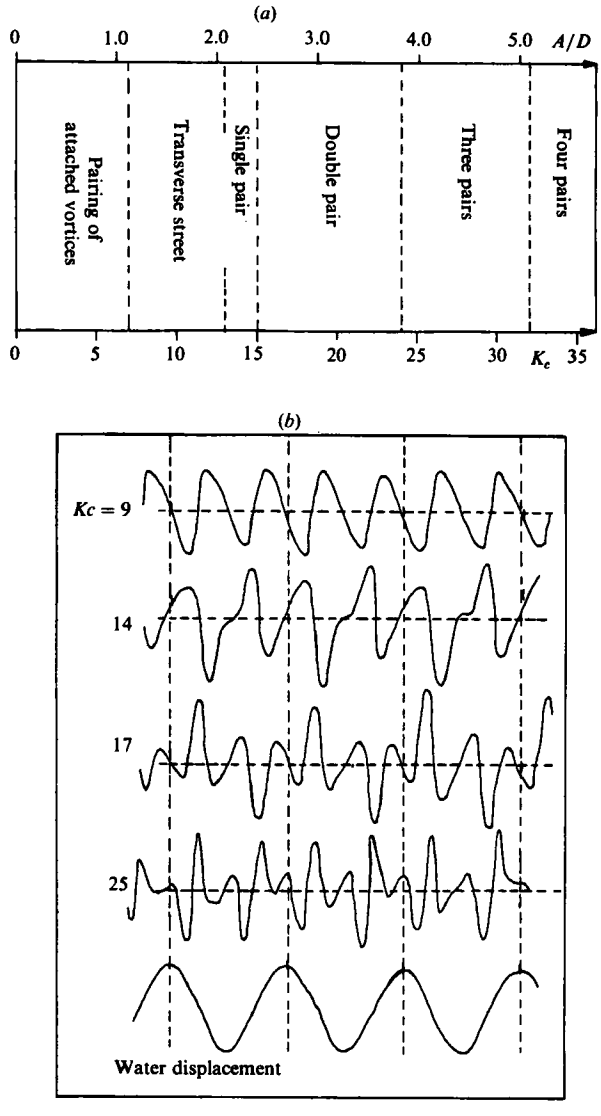

FIGURE 3. (*a*) A rough guide to the ranges of Keulegan–Carpenter number (or amplitude/diameter) corresponding with each flow pattern. (*b*). Typical near-regular lift-force fluctuations for a range of Keulegan–Carpenter numbers. Each regular lift-force profile represents a repeatable vortex wake pattern, demonstrated in §3.

cylinder motion, although for simplicity in this case our view of the vortices is made through a framework which moves with the cylinder.

3.1.1. *Pairing of attached vortices* ($0 < Kc < 7$)

In this range of flow amplitudes, a pair of small 'attached' vortices form in the wake of the cylinder in each half cycle resembling the vortex pair formed behind a cylinder in a starting flow. When the cylinder reverses direction, the attached vortices split up and pair with new vortices in the new half cycle, thus convecting away from the local flow region around the cylinder. This pairing of attached vortices occurs only at the time of flow reversal between small vortices which were still attached to the

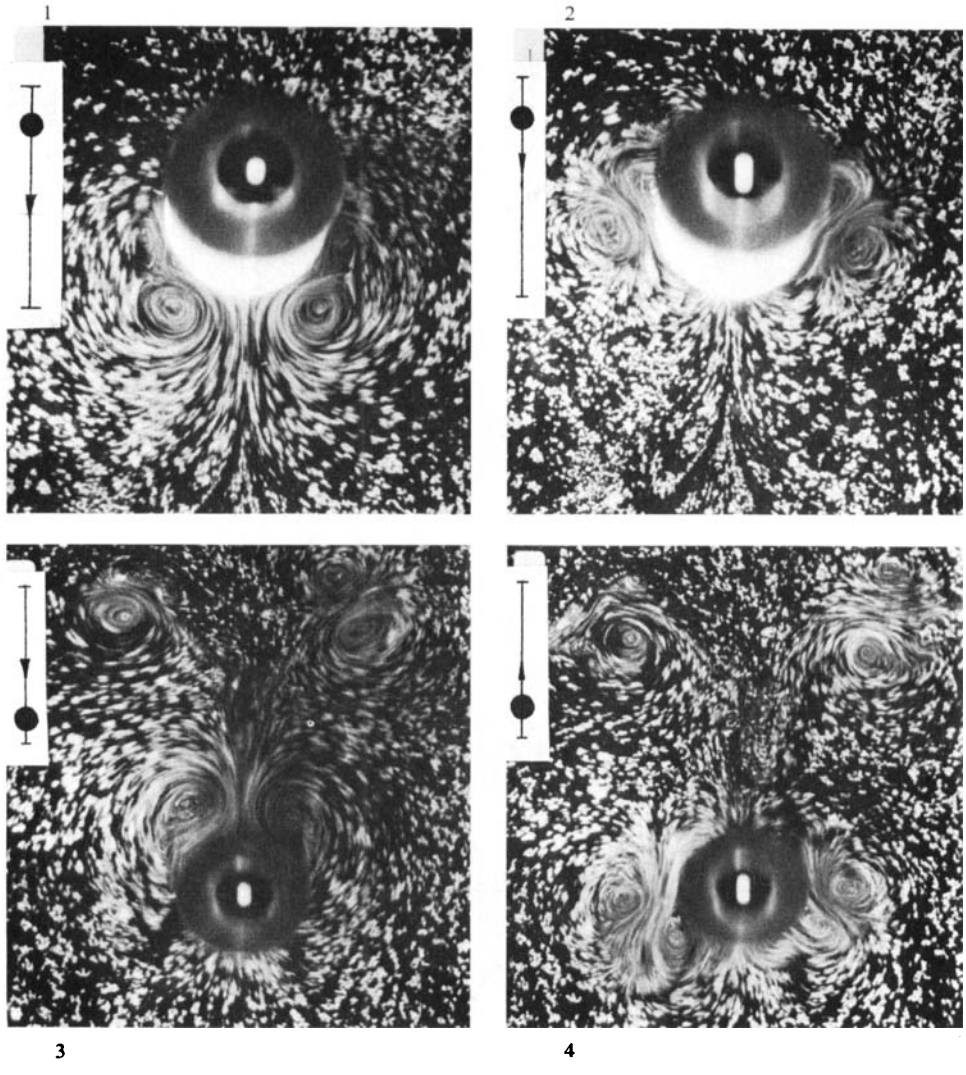

FIGURE 4. Symmetric pairing of attached vortices for $Kc < 4$. Arrows refer to the cylinder motion. Small-wake vortices form pairs as the cylinder reverses direction.

cylinder just prior to flow reversal. Such a process is demonstrated from visualization in figure 4 soon after the beginning of cylinder oscillations. In (1) the attached eddies (from a previous half cycle) are split up as the cylinder moves downwards, and in (2) they each form a small vortex pair with new small vortices. These small pairs formed at flow reversal are shown in the top corners of (3) and (4), where the cylinder reverses again and this eddy pairing repeats itself. The pairing is reasonably symmetric up to about $Kc = 4$, in that the two pairs are formed simultaneously when the flow reverses. Between $Kc = 4$ and 7, the attached vortices become unequal in strength and the vortex pairs do not form simultaneously upon flow reversal, giving rise to a lift force of low amplitude fluctuating at the oscillation frequency.

3.1.2. *Transverse street/single pair* ($7 < Kc < 15$)

This flow regime is the most repeatable of the patterns, and represents the shedding of one large vortex during each half cycle. For these amplitudes we see the pairing

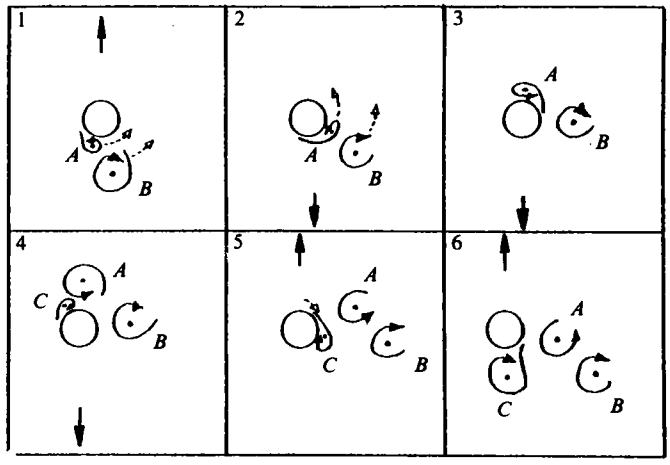

(*a*)

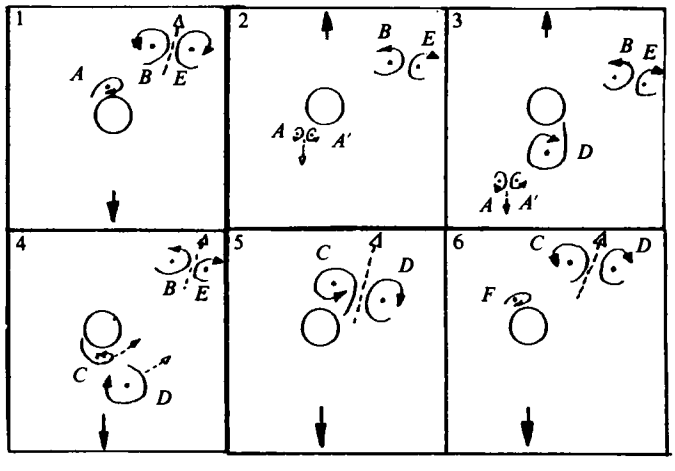

(*b*)

FIGURE 5. (*a*) Transverse street for $7 < Kc < 13$. (*b*) Single pairs for $13 < Kc < 15$. The arrows refer to cylinder motion but the vortices are viewed from a reference frame which moves with the cylinder. In (*a*) the wake consists of a series of vortices convecting out to one side of the cylinder in the form of a jet or street. In (*b*) the wake consists of a series of pairs convecting away each cycle at around 45° to the flow oscillation direction, and on one side of the cylinder only.

of 'shed' vortices, rather than the pairing of 'attached' vortices in §3.1.1. The transverse street is composed of a street or 'jet' of vortices moving away from the local-flow region of the cylinder, roughly perpendicular to the oscillation direction. The process of shedding and pairing that forms such a street is demonstrated in figure 5(*a*), where the arrows refer to the motion of the cylinder, and for simplicity our reference frame now moves with the cylinder. At the end of a half cycle in (1) the wake close to the cylinder consists of a shed vortex B and an unshed vortex A which may both move round the cylinder on the same side during cylinder reversal (in this case the right-hand side). Due to the greater induced fluid velocities on the right-hand side of the cylinder because of the presence of vortex B, this then becomes

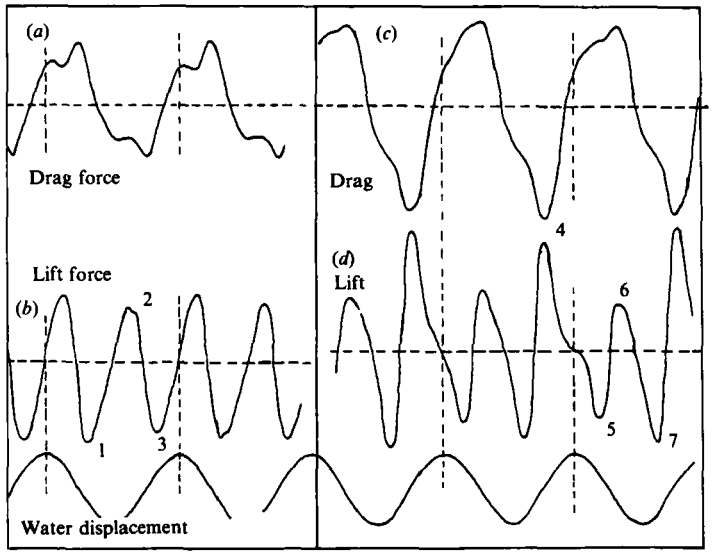

FIGURE 6. Typical shapes of lift and in-line force fluctuations for the regime $7 < Kc < 15$ taken from the U-tube. In (*a*) and (*b*) are force records from the transverse street wake at $Kc = 11.0$, while in (*c*) and (*d*) are records for the single-pair wake at $Kc = 13.7$. Horizontal dashed lines indicate zero force levels.

the 'preferred' side for the next vortex to be shed. Vortex A amalgamates with more vorticity of the same sign, and pairs with vortex B. Vortex A sheds in (4) in a similar manner to vortex B in (1), and the resulting wake in (6) is a series of alternate vortices convecting away from the local-cylinder region under their induced velocities in the form of a street. This kind of vortex pairing, as the cylinder sweeps past a previous half-cycle wake, is fundamental to all the observed wake patterns.

At the upper end of this range of amplitudes (between $13 < Kc < 15$) the main vortex pattern comprises a series of pairs convecting away from the cylinder at roughly 45° to the cylinder-oscillation direction, as shown schematically in figure 5 (*b*). The attached (or unshed) vortex A at the end of a half cycle in (1) pairs with a small vortex A' at flow reversal in (2) and (3), in a manner similar to the pairing of attached vortices in §3.1.1. The larger and more significant vortex D moves round on the same side of the cylinder as the unshed vortex C at the next flow reversal. Vortex C amalgamates with more vorticity of the same sign and coupled with vortex D they form one of the main vortex pairs. Thus the large pair C and D follow the pair $B+E$ formed a cycle earlier, and so on. In both the transverse-street and single-pair wakes, the vortices tend to convect out to one side predominantly. Initial conditions determine which side is favoured, although the shedding can intermittently change sides.

These patterns of shedding may possibly be of significance to offshore fluid loading because they are remarkably repeatable, and can induce an almost regular lift-force oscillation. Examples of lift- and in-line-force traces from a transverse street wake are shown in figures 6 (*a*) and (*b*), respectively. In this case the forces are measured from the U-tube and therefore the in-line force includes the pressure-gradient component in-phase with the fluid acceleration. Using the same scale for each force it is evident that the lift-force amplitude can exceed the in-line-force amplitude. The same is true for force traces from a single-pair wake in (*c*) and (*d*) showing in-line force

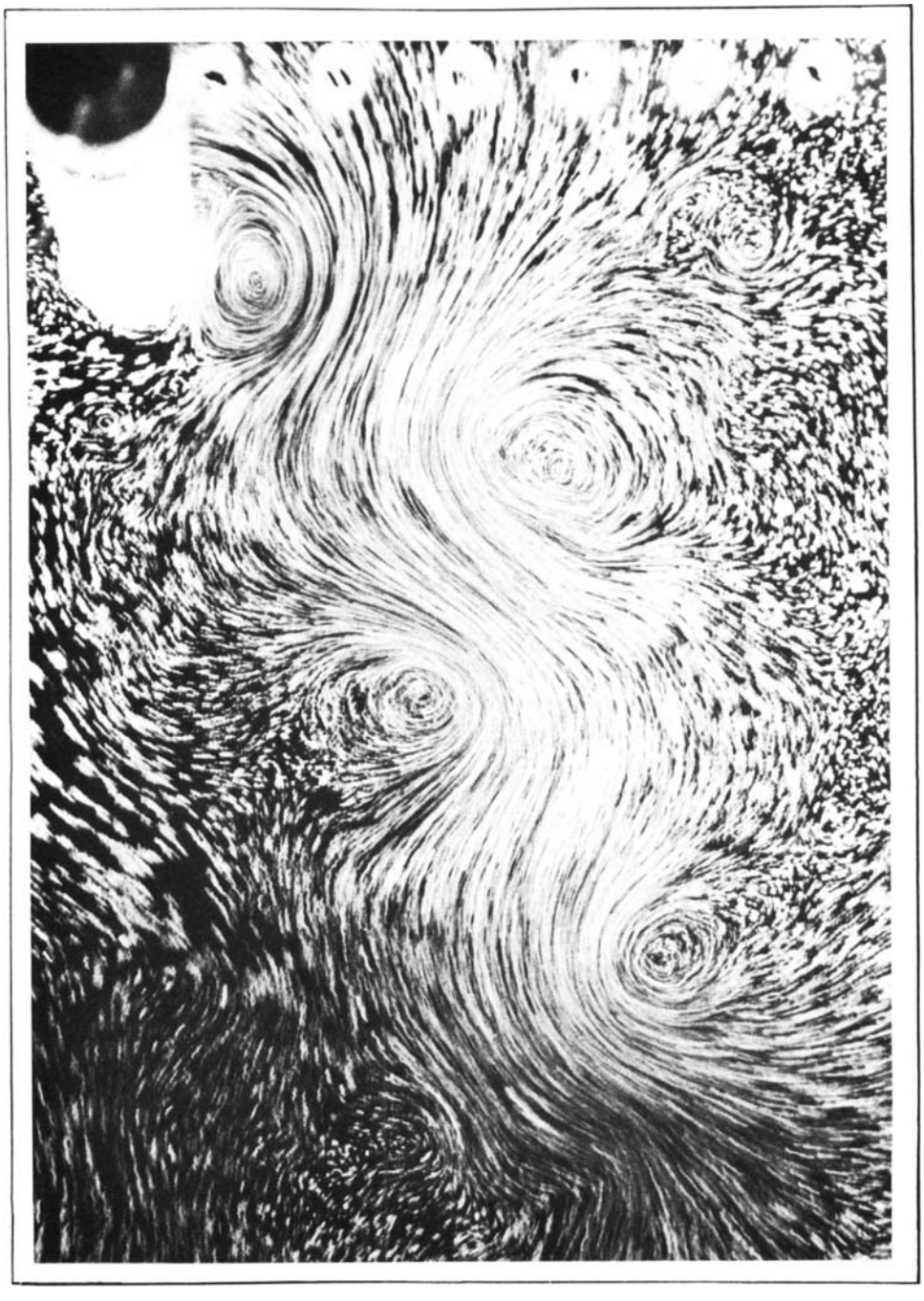

FIGURE 7. Transverse-street wake for $Kc = 12.0$. In this photograph the cylinder is moving to the left, and is near the end of a half cycle. Due to the induced velocities of the main vortices, one of which is shed in each half cycle, the trail of vortices convects away at around 90° to the oscillation direction in the form of a street. In this case the street travels downwards.

and lift respectively. Each negative peak marked 1 and 3 in (*b*) is caused by the growth and shedding of a large vortex (such as *B* and *A* in figure 5(*a*)) in each half cycle. The peaks are of the same sign because, from (2), the lift is found from the rate of change of the product of vortex circulation Γ and position x parallel to the oscillation direction, i.e. lift $\propto -\partial/\partial t(\Gamma x)$. The positive peaks in figure 6(*b*) (for example marked 2) are induced by the return of the most recently shed vortex towards the cylinder just after flow reversal. As a rough rule the fundamental lift frequency is $(n+1)$ times the oscillation frequency, where n is the number of vortices shed per half cycle; hence the lift frequency here is twice the oscillation frequency. For the single-pair wake the lift- and in-line-force oscillations in (*c*) and (*d*) are clearly non-symmetric in that the force in one half cycle is not equal and opposite to the force one half cycle earlier. The simultaneous occurrence of a large positive peak in the lift (at 4) and the negative peak in the in-line force are induced in the half cycle when a large vortex, such as *C* in figure 5(*b*), grows and is shed. It is interesting to note in figure 6(*b*) the existence of a small mean-lift force due to the convection of the wake vortices out to one side of the cylinder.

Clear visualization of a transverse street is shown in figure 7 for $Kc = 12.0$ where the street is moving downwards at roughly 90° to the motion of the cylinder (across the page). This vortex configuration has a striking resemblance to a Kármán street, except that here the motion of the alternate vortices and the jet of fluid between them are directed away from the cylinder rather than towards it.

The visualization in figure 8(*a*) for slightly larger amplitudes ($Kc = 13.5$) clearly demonstrates the generation of a large pair of vortices near the end of a half cycle when the cylinder translates from left to right. The clockwise vortex on the right was shed during the previous half cycle and pairs with the anticlockwise vortex on the left forming in the present half cycle. For this particular example, a new vortex pair is formed in each cycle and convects to the left and upwards from the cylinder at around 45° to the cylinder-oscillation direction.

In order to compare visualization fixed with respect to the undisturbed fluid in figure 8(*a*) with visualization fixed with respect to the cylinder, the photograph in figure 8(*b*) from the U-tube is shown. In the latter visualization for the transverse-street wake at $Kc = 11.0$, polystyrene beads are observed around a mid-section of the cylinder. The flow is travelling to the left past the fixed cylinder and an anticlockwise vortex has just been shed and is to the left of the cylinder. The exact position of a clockwise vortex (formed one half cycle earlier) about 2 diameters above the cylinder is obscured by the motion of the bulk of the fluid. The masking of the vortex motions by a superposed stream velocity is typified by such visualization, and thus demonstrates how such a reference frame is less effective than visualization fixed with respect to the undisturbed fluid.

3.1.3. *Double pair* ($15 < Kc < 24$)

As the flow amplitudes increase, so the single-pair pattern merges into a 'double-pair' wake. The latter wake comprises the shedding of two large vortices in each half cycle, and the formation of two pairs in each cycle. A series of vortex pairs convect away from the cylinder in opposite directions and from opposite quadrants. A schematic diagram showing the sequence of shedding in figure 9(*a*) shows, for example, a vortex pair (*M*, *N*) formed in one half cycle downwards and out to the left of the cylinder in (2) and (3). In the following half cycle a pair (*P*, *Q*) convects away upwards and to the right relative to the cylinder in (4) and (5).

A schematic lift-force oscillation in figure 9(*b*) for this double-pair wake corresponds

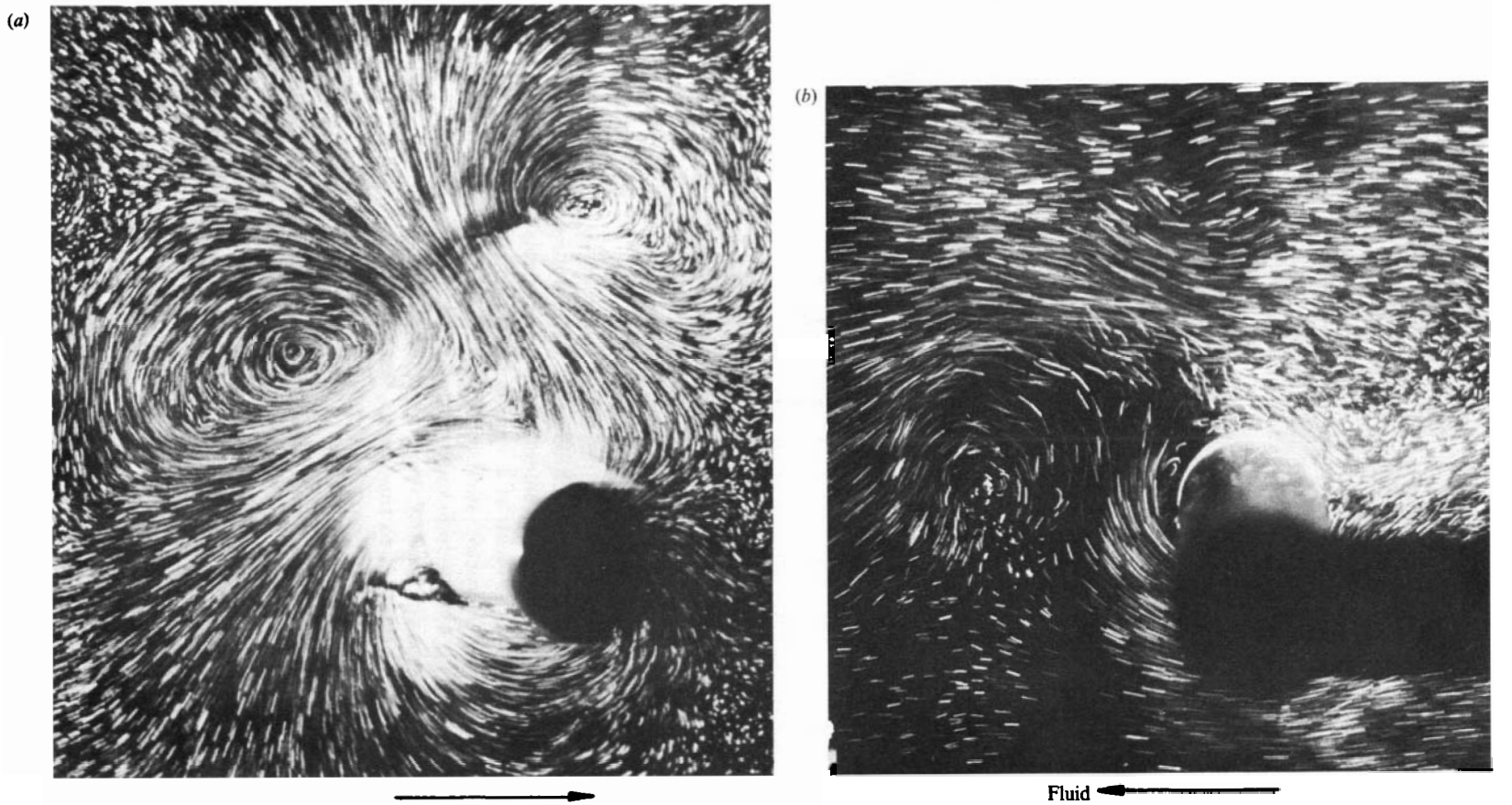

FIGURE 8. (*a*) Single-pair wake for $Kc = 13.5$. This photograph clearly demonstrates the generation of a large pair of vortices near the end of a half cycle of oscillation, with the cylinder moving from left to right. The clockwise vortex on the right was shed during the previous half cycle and induced the shedding of the anticlockwise vortex on the left in the present half cycle. Such vortex pairing is fundamental to observed wake patterns in oscillatory flow. (*b*) Transverse street for $Kc = 11.0$. This photograph is taken from the U-tube where visualization is fixed with respect to the cylinder. Flow is to the left, and is near the end of a half cycle. An anticlockwise vortex has just been shed from the cylinder and is to the left of it.

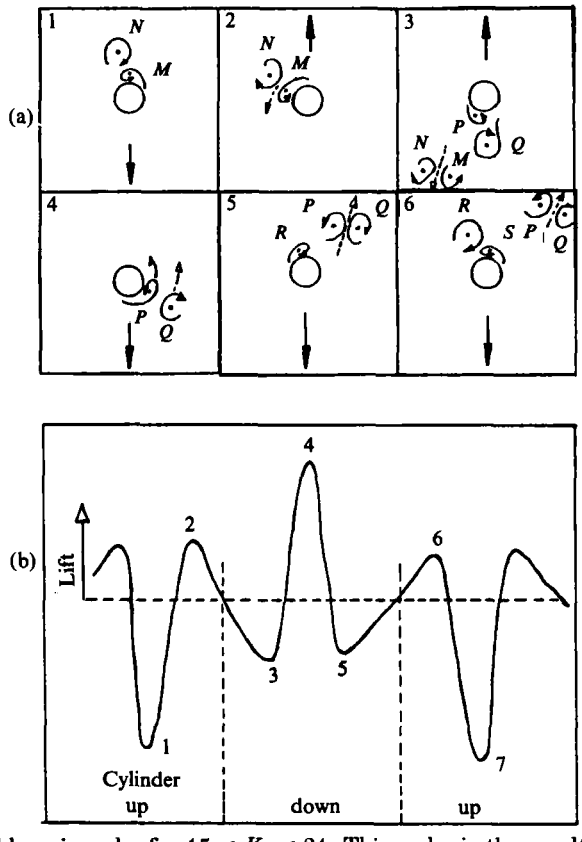

FIGURE 9. (*a*) Double-pair wake for $15 < Kc < 24$. This wake is the result of two vortices being shed in each half cycle. Two trails of vortex pairs convect away from the cylinder in opposite directions and from opposite sides of the cylinder (for example vortices $N+M$ and $P+Q$). (*b*) Diagram showing the shape of a typical lift-force oscillation. The fundamental lift force associated with such vortex motions is at three times the oscillation frequency.

with the vortex pattern in figure 9(*a*) as follows. If we denote positive circulation (Γ) as anticlockwise, and positive displacement (x) of a vortex relative to the cylinder as downwards, then the negative peak at 1 can be shown to correspond with both the growth and shedding of a vortex such as M. Again, we can consider the lift proportional to $-\partial/\partial t\,(\Gamma x)$, and include only the motions of the strongest vortices close to the cylinder. The maximum at 2 corresponds with the growth and shedding of vortex Q, and the minimum at 3 to the vortex Q returning towards the cylinder as the flow reverses. Similarly, in the next half cycle, the shedding of vortices P and R cause the maximum at 4 and the minimum at 5 respectively, and so on. We can therefore conclude that the force trace for $Kc = 17$ in figure 3(*b*) indicates the existence of a double-pair wake. The fundamental lift frequency is now three times the cylinder-oscillation frequency.

A demonstration of such a vortex wake from visualization is shown in figure 10 where the cylinder moves across the page. In (1) a vortex pair is formed (from a previous and present half-cycle vortex) and in (2) this pair convects upwards and to the right of the cylinder which is travelling to the left. In the following half cycle a pair forms in (3) and will convect away downwards and to the left of the cylinder in (4).

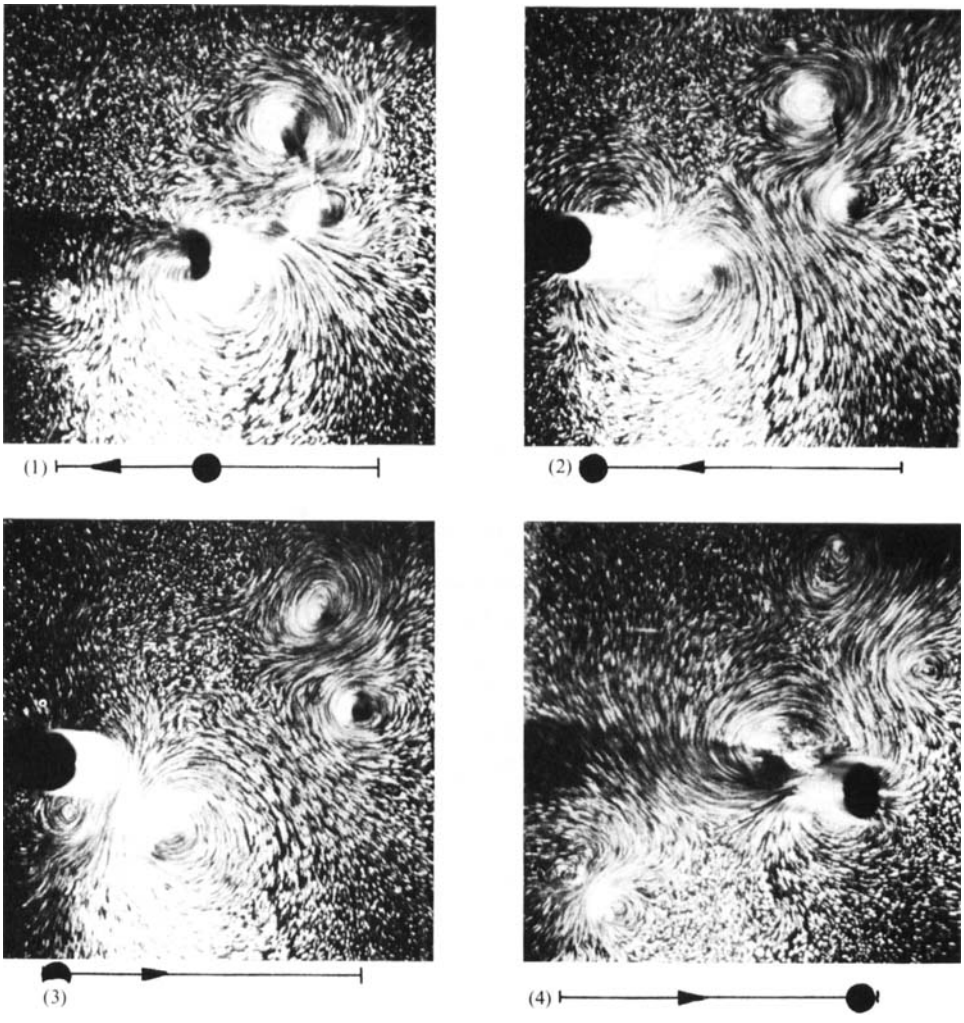

FIGURE 10. Double-pair wake at $Kc = 16$. The wake comprises the formation of a vortex pair in each half cycle. Vortex pairs convect away upwards to the right, and also downwards to the left of the cylinder.

3.1.4. *Three pairs* ($24 < Kc < 32$) *and four pairs* ($32 < Kc < 40$)

As the oscillation amplitudes are increased still further, so the number of shed vortices in a half cycle increases and, in the range $24 < Kc < 32$, there are predominantly three vortices shed in each half cycle. In figure 11 (*a*) we can see that three pairs of vortices are formed in each half cycle, causing the schematic lift-force oscillation in figure 11 (*b*). In (1) the vortices A and B shed in this half cycle have paired with vortices A^* and B^* shed in the previous half cycle. As the cylinder reverses direction in (2), vortex C pairs with vortex D and when B from the previous half cycle sweeps past the cylinder in (3) and (4) it pairs with E. In (5) and (6) as the flow reverses again, F is left to pair with G in the new half cycle. As with the double-pair wake, the shedding and motions of each large vortex causes a particular peak in the lift force depending on the magnitude and sign of $-\partial/\partial t(\Gamma x)$. For

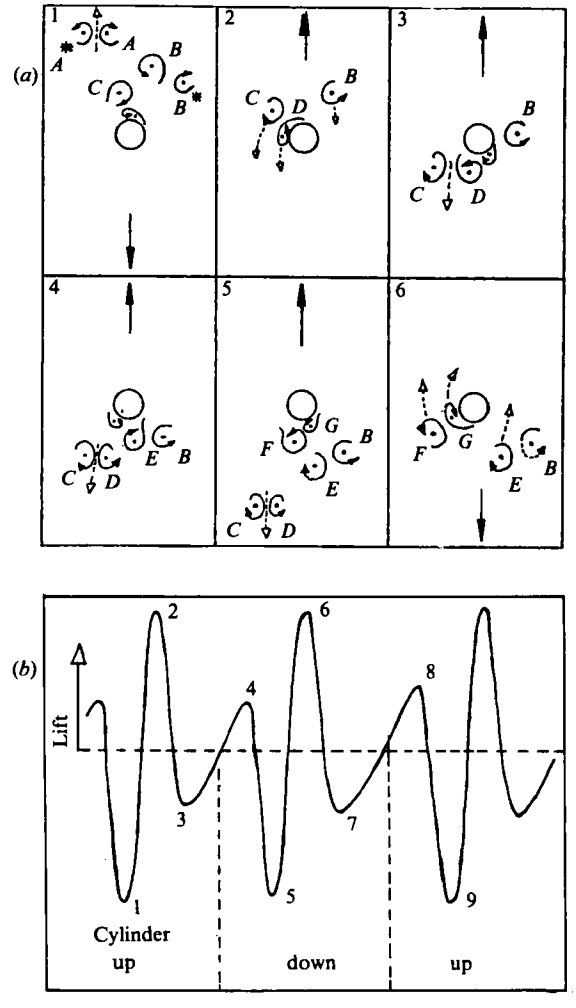

FIGURE 11. (*a*) Three-pairs wake for $24 < Kc < 32$. This wake is the result of three vortices being shed in a half cycle, and comprises three vortex pairings in a cycle (for example vortices $C+D$, $B+E$ and $F+G$. (*b*) Diagram showing the shape of a typical lift-force oscillation. The fundamental lift-force frequency associated with these vortex motions is at four times the oscillation frequency.

example, the growth and shedding of vortices D, E and F cause the peaks 1, 2 and 3 respectively. The return of F towards the cylinder causes the maximum at 4, followed by the minimum at 5 due to the formation of vortex G, and so on. The lift-force oscillation is similar in each half cycle because, for example, vortices D and G (the latter formed a half cycle after D) both give the same sign of $-\partial/\partial t\,(\Gamma x)$. This flow pattern is responsible for the actual lift oscillations for $Kc = 25$ in figure 3(*b*), and the fundamental lift frequency is now four times the oscillation frequency.

Flow visualization of this wake for one half cycle is shown in figure 12, when the cylinder moves from right to left through a previous half-cycle wake. The sequential photographs demonstrate one pair forming in (2) and (3) from the upper side, and another pair forming in (4) and (5) from the lower side, with a third shed vortex from the upper side near the cylinder in (5) and (6).

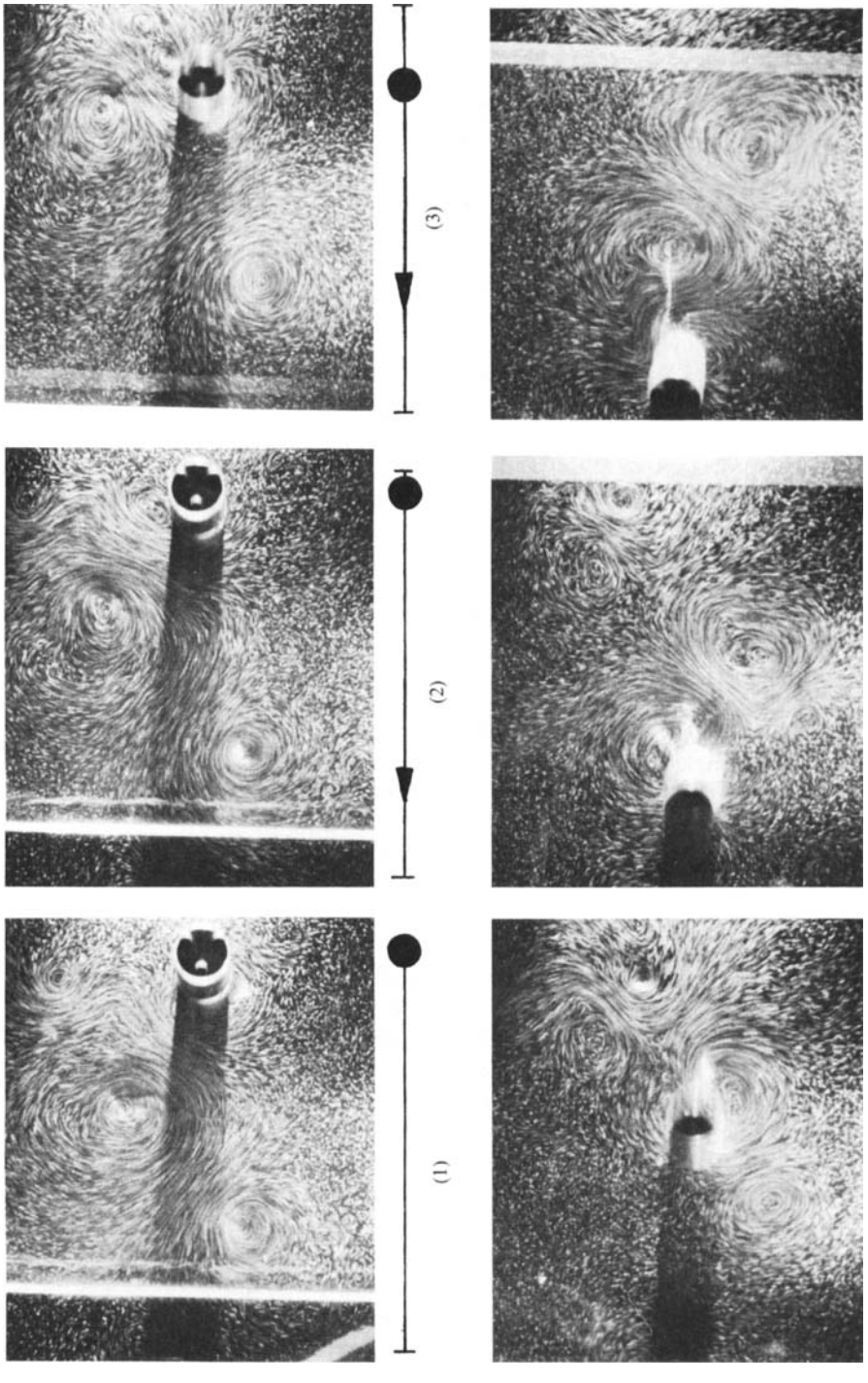

FIGURE 12. Three-pairs wake at $Kc = 27$. The sequential photographs demonstrate the process of vortex pairing in one half cycle as the cylinder sweeps through its previous half-cycle wake.

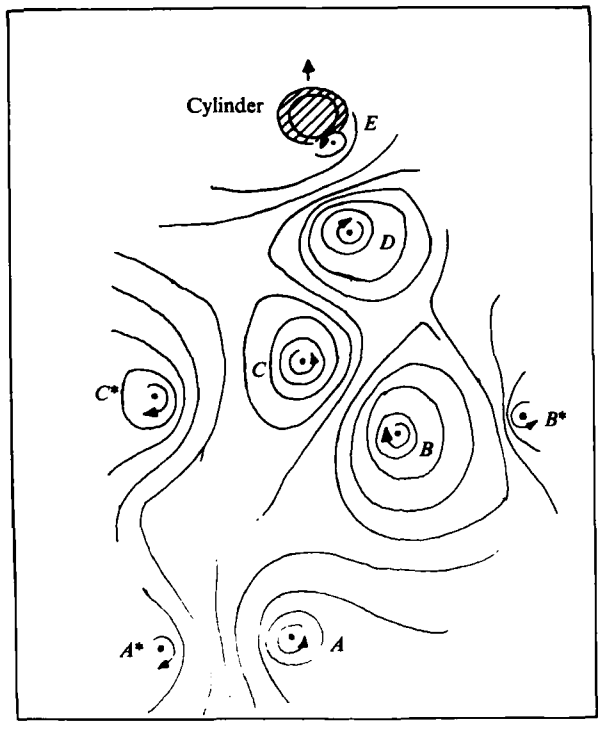

FIGURE 13. Four-pairs wake at $Kc = 33$. This diagram is taken from a photograph and indicates the instantaneous direction of motion of the surface particles. At the end of one half cycle the cylinder has moved upwards through the wake of a previous half cycle. Successive half-cycle wakes are pushed apart into parallel regions on either side of the path of the cylinder oscillations.

In the range ($32 < Kc < 40$), a further system of pairings occurs, in this case forming 4 pairs of vortices in a full cycle, and a fundamental lift force of five times the oscillation frequency. A schematic diagram of the instantaneous direction of motion of the particles taken from a photograph of such a wake near the end of a half cycle is shown in figure 13. Each vortex marked with an asterisk such as A^* from the previous half cycle has paired with vortices such as A in the present half cycle. Again, typical lift oscillations could be understood by consideration of the values of $-\partial/\partial t\,(\Gamma x)$ for the strongest vortices nearest to the cylinder.

For larger flow amplitudes such wake patterns and regular lift oscillations become less repeatable, and the fundamental lift frequencies increase as more vortices are shed per cycle.

In each of the patterns described in §3.1.1 to §3.1.4, the process of vortex pairing between a previous half-cycle vortex with one in a present half cycle is fundamental. Such pairing is the cause of the continuity of the wake patterns and thus the cause of the regular lift oscillations and fundamental frequencies demonstrated above. In general, only the vortices of a previous and present half cycle retain their importance in the fluid forces on the cylinder. Vortices may 'escape' from the local-flow region by forming pairs which convect away from the local-cylinder region. At low amplitudes ($Kc < 7$) the small vortices are subject to a combination of mixing with opposite-signed vorticity close to the cylinder when the flow reverses, and to convection of vorticity away from the cylinder as shown in figure 4. Where one or two large vortices are shed per half cycle ($7 < Kc < 24$), the pairing process convects

the vortices away from the local cylinder region sometimes at large angles to the oscillation direction. For larger amplitudes, as the cylinder sweeps back through a previous half cycle wake, the first vortex pair convects away rapidly roughly in line with the oscillation direction. Subsequently, the previous half-cycle wake is pushed apart to either side of the present half-cycle wake as shown for example in figure 13, as though sequential layers of vortices are pushed into parallel regions lying to either side of the path of cylinder oscillations. However, it is difficult at these amplitudes to visualize vortices that have been shed one or more cycles earlier. These previously shed vortices are possibly weakened by mixing with opposite-signed vorticity and by three-dimensional destruction of the vortices.

It is not known how these vortex patterns for a single cylinder are affected by a variation of Reynolds number, although it is expected that these regimes will remain roughly similar over the range of subcritical Reynolds numbers. However, there is little evidence as yet to show that such vortex-shedding patterns occur at supercritical Reynolds numbers.

3.2. *Hydrodynamic interference for a pair of cylinders*

The oscillations of two neighbouring cylinders in the tank can promote certain modifications to the flow patterns and induced forces that were identified in §3.1 for an isolated cylinder. For moderate spacing between the cylinders (compared to the oscillation amplitudes) the vortex shedding can synchronize in phase or in antiphase. When the cylinders are even more tightly packed, the wake may form as though it is created by a single large body, sometimes through the action of vortex amalgamation. Such flow interference can have significant effects on the induced forces on the cylinders, in some cases causing a marked increase of the lift or the in-line force.

In the following §3.2.1 the case of two cylinders oscillating in the transverse-street/single-pair regime (identified for a single cylinder in §3.1.2) is investigated. For these amplitudes one main vortex is shed per half cycle, and the lift-force magnitude is found to be comparable to the in-line force. Some of the features of the flow around two cylinders for this regime are found later to occur at higher amplitudes, see §3.2.2.

3.2.1. *Transverse-street/single-pair regime* ($7 < Kc < 15$)

In this regime the vortex flow patterns are markedly influenced by flow interference for moderate to small spacings. Vortex shedding is found to be predominantly in-phase for two cylinders in-line, and in antiphase for cylinders at 45° or side by side. For all three orientations at sufficiently small gaps ($g^* < 0.5$) the wake becomes roughly that due to a larger solid body. Typical vortex wake configurations are demonstrated schematically in figure 14.

The overall wake of two cylinders side by side in figure 14(*a*) consists of a pattern of vortex pairs convecting away from the local-cylinder region parallel with the oscillation direction. The synchronous shedding of two large vortices from the gap sides of the two cylinders in every half cycle forms a vortex pair, and such shedding is found to be remarkably repeatable. This wake is very different from the transverse wake found for an isolated cylinder at the same flow amplitudes. The formation of these 'symmetric' pairs from between the cylinders is shown from flow visualization in figures 15(*a*) and (*b*), for $Kc = 14$. The cylinders are translating downwards in (*a*) for $g^* = 1.5$ soon after the oscillations were commenced, clearly showing a vortex pair above the cylinders convecting away upwards and a pair below convecting away downwards. The general streaming of fluid in from the sides and away from the cylinders in both directions parallel with the oscillation direction is shown in (*b*) for

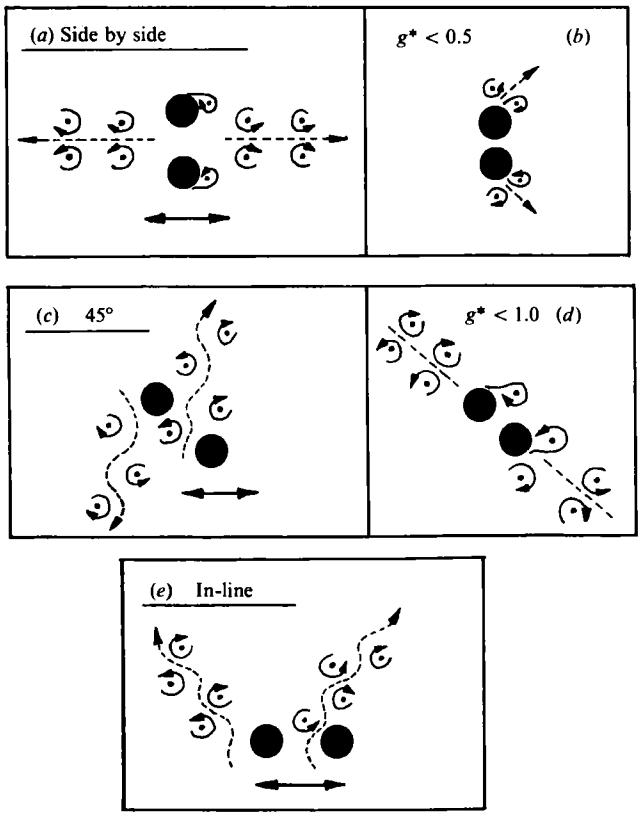

FIGURE 14. Influence of cylinder proximity on the vortex wakes in the transverse-street regime ($7 < Kc < 15$). Cylinders are side by side in (*a*) and (*b*). Cylinders are at 45° in (*c*) and (*d*). Cylinders are in-line with the oscillations in (*e*).

$g^* = 2.0$ after a large number of cycles. For very small cylinder gaps in figure 14(*b*) the cylinder pair behaves as a larger solid body, with small vortex pairs shed at flow reversal from the outside edges of the cylinders.

For two cylinders at 45°, the vortex shedding tends to synchronize in antiphase in the range of gaps, $1.0 < g^* < 3.0$. The overall wake is shown schematically in figure 14(*c*), where the vortices convect away from the two cylinders in the form of two transverse streets flowing in opposite directions. Flow visualization of such a wake is shown in figure 15(*c*) for $Kc = 14$ when the cylinders have travelled from left to right near the end of a half cycle. The flow diagram in (*d*) shows the instantaneous direction of motion of the particles visualized in (*c*) and demonstrates the two jets of fluid flowing in opposite directions both perpendicular to the oscillation direction. When $g^* < 1.0$ in figure 14(*d*) an important change in the vortex wake occurs. The wake becomes a series of vortex pairs convecting away from the local region at around 45° to the oscillation direction. The convection direction of the pairs is naturally biased to lie parallel to the line joining the cylinder centres. This 'double-pair' wake is significant in that it becomes predominant for moderate spacings up to surprisingly large flow amplitudes (up to $Kc \simeq 30$) and induces large peaks in the lift force on each cylinder.

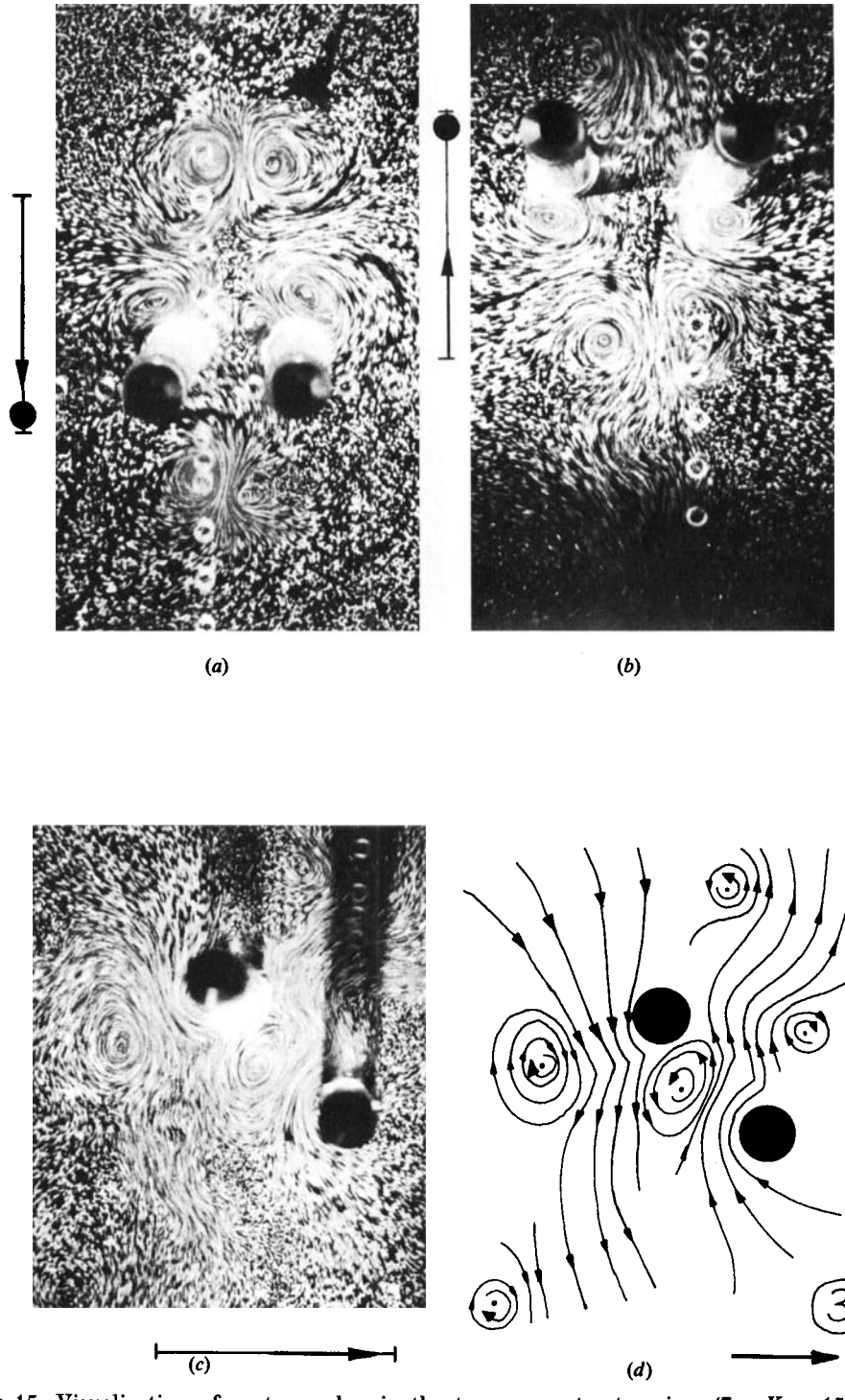

FIGURE 15. Visualization of vortex wakes in the transverse-street regime ($7 < Kc < 15$). The cylinders in (*a*) and (*b*) are side by side, with $g^* = 1.5$ and 2.0 respectively, creating a system of vortex pairs convecting away from the cylinder parallel to the oscillations. The oscillation of cylinders at 45° in (*c*) and (*d*) with $g^* = 2.0$ causes two vortex streets to flow in opposite directions owing to antiphase shedding.

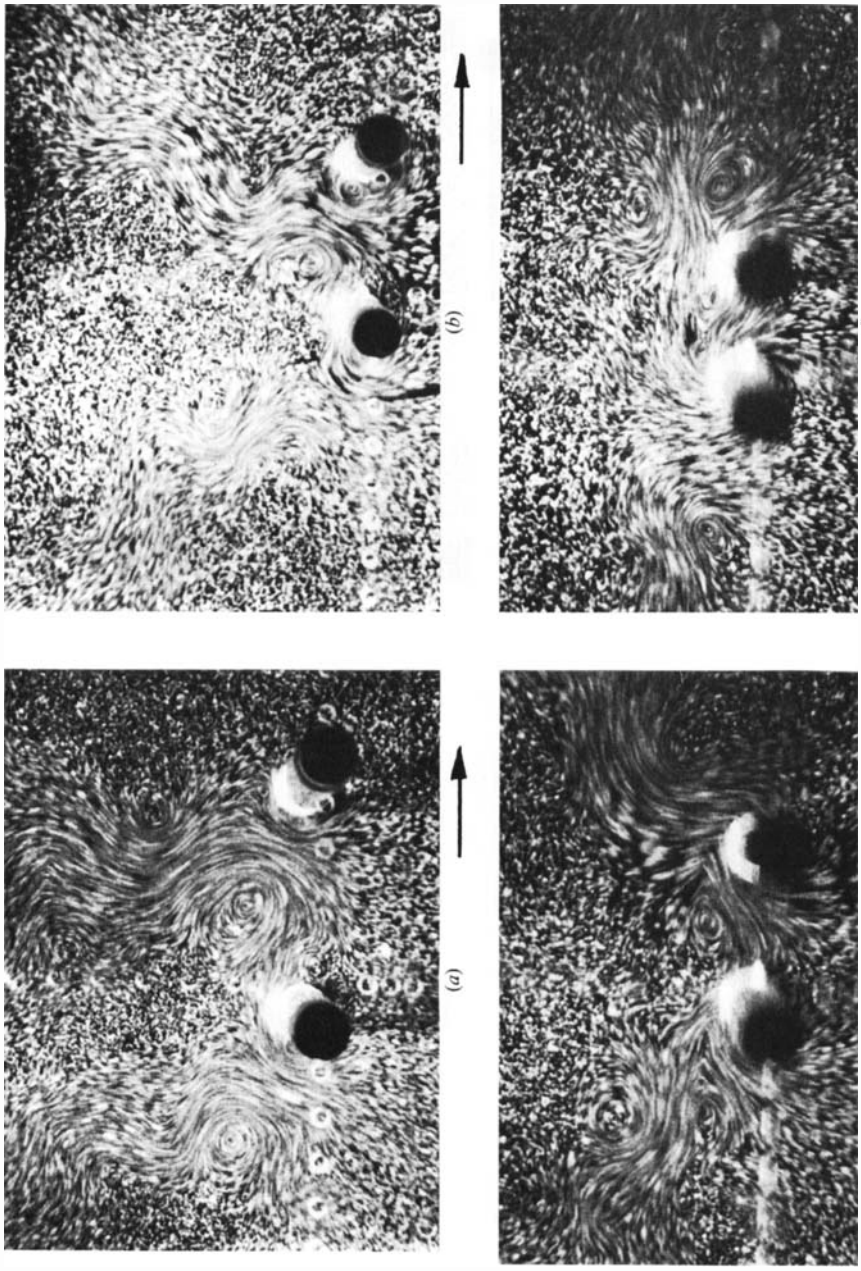

FIGURE 16. Visualization of a cylinder pair in-line with the oscillation direction in the transverse-street regime ($7 < Kc < 15$). Both streets convect upwards as the cylinders oscillate across the page at $Kc = 14$. A small phase difference in the shedding increases as the cylinders become closer, and causes the streets to diverge. If we define α as the angle between each street direction and a line perpendicular to the oscillations then in (*a*) $g^* = 4.0$, $\alpha = 0°$; (*b*) 3.0, 35°; (*c*) 2.0, 50°; (*d*) 1.0, 90°.

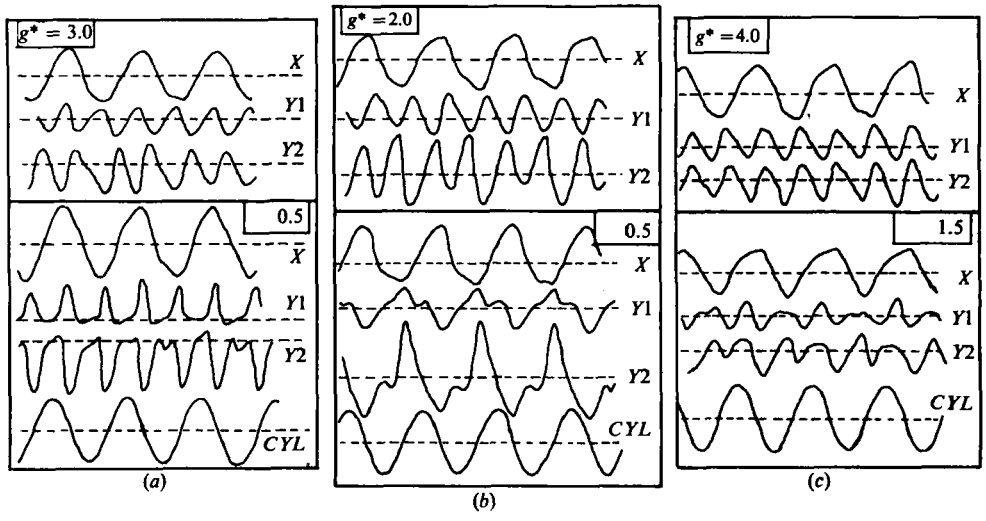

FIGURE 17. Force traces on each cylinder for $Kc = 13.2$ in the transverse-street regime. In (*a*) the cylinders are side by side, in (*b*) they are at 45° and in (*c*) the cylinders are in-line with the oscillations. An explanation of each force record (X, $Y1$, $Y2$) is included in the text. Horizontal dashed lines indicate zero force levels.

For the case of two cylinders in-line with the relative flow, the vortex shedding tends to synchronize close to in-phase for $g^* < 4.0$ so that the wake comprises two transverse streets both flowing out to one side as shown in figure 14 (*e*). As g^* reduces so the vortex shedding of the downstream cylinder in each half cycle slightly leads that of the upstream cylinder. This small phase lead causes the vortex streets from each of the cylinders to be angled to each other. Such a wake may be seen from visualization in figure 16. In (*a*) the streets are roughly parallel to each other and perpendicular to the oscillation direction. As gaps are reduced in (*b*) and (*c*) so the streets diverge, until in (*d*) for $g^* = 1.0$ the wake vortices convect away in-line with the cylinder oscillation direction. Interestingly this latter wake is similar to that for two cylinders side by side. For very small gaps the vortex shedding in each half cycle takes place only in the rear of the downstream cylinder, and no specific vortex pattern has been observed here.

Typical force profiles for the above vortex patterns are shown in figure 17. Cylinders 1 and 2 refer to those cylinders in figure 2 where positive lift and in-line-force directions are defined. The amplification of the lift signal for $Y2$ is about 1.6 times the amplification of signal $Y1$, and the latter signal amplification is the same as that for the in-line force X (measured from cylinder 2). However, the scale for $Y1$ is the same throughout the figure (*a*, *b* and *c*), and likewise for X and $Y2$. Each force trace corresponds with the cylinder displacement CYL marked below them. Although only limited time histories can be shown here (and also in figure 21 later) the phase relationships between lift-force signals are repeatable for large numbers of cycles, especially for the signals recorded at low spacings. At $g^* = 3.0$ in (*a*) for the side-by-side arrangement, the lift and drag is roughly that which is found for isolated cylinders. However, the lift profiles of each cylinder are in antiphase, indicating the antiphase vortex shedding demonstrated above. For a small gap, $g^* = 0.5$, the in-line force is magnified, and the cylinders experience a large mean repulsive lift force. The peaks

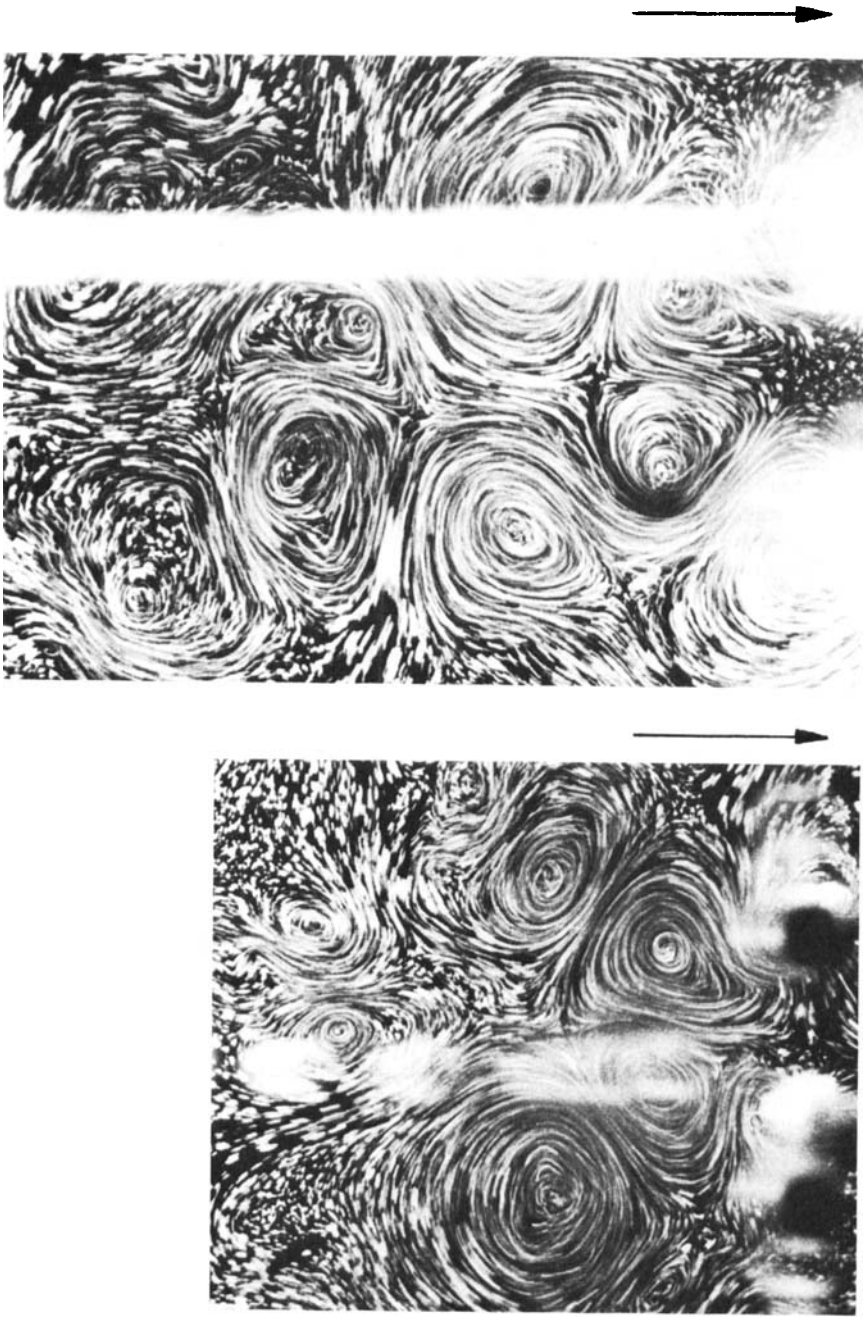

(a) (b)

FIGURE 18. Visualization of cylinder pairs side by side at $Kc = 24, g^* = 1.0$, in (*a*), and at $Kc = 54, g^* = 2.0$ in (*b*). Vortex shedding is in antiphase between the cylinders and forms a half-cycle wake which is symmetric with respect to the centreline of the wake. In both (*a*) and (*b*) the wake centreline is vertical and between the cylinders which are translating downwards at the lower end of each photograph.

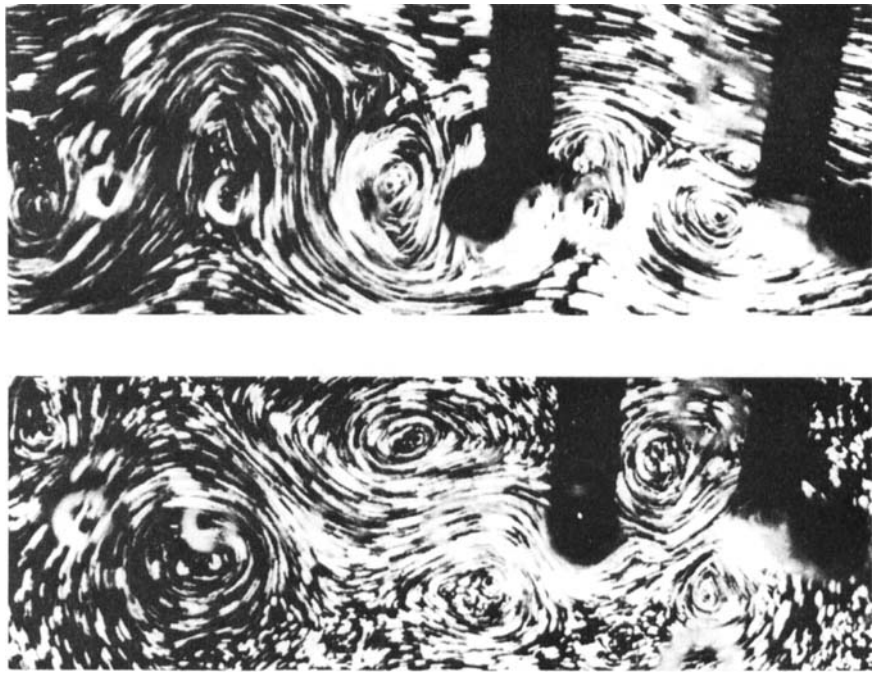

(*a*)

(*b*)

FIGURE 19. Visualization of cylinder pairs in-line with the oscillation direction at $Kc = 54$. The cylinders are moving to the right in (*a*) when $g^* = 3.0$, and also to the right in (*b*) near the end of a half cycle when $g^* = 2.0$. Under these conditions the upstream-cylinder wake flows round the downstream cylinder, to form the basis of the vortex wake downstream of both cylinders.

in the lift force profiles when $g^* = 0.5$ occur as the gap pairs are shed in each half cycle. The force profiles in (*b*) for two cylinders at 45° show antiphase lift at $g^* = 2.0$, and a magnified lift for $g^* = 0.5$ when the combined wake of the cylinders is the double-pair pattern. The large lift peak occurs when one of the vortex pairs is formed and convected away, so that each cylinder experiences these large peaks in alternate half cycles. The asymmetry in the in-line force profile for the 45° orientation is also evident for the in-line arrangement in (*c*). In this diagram the in-phase lift profiles for both $g^* = 4.0$ and 1.5 reflect the in-phase vortex shedding. Several features of the flow and forces found for a cylinder pair oscillating in the above regime occur also at higher amplitudes.

3.2.2. *Flow interference when* $Kc > 15$

(i) *Two cylinders side by side.* When the cylinders are arranged side by side the vortex shedding is predominantly in antiphase for all amplitudes tested (up to $Kc = 55$) when $g^* < 4.0$. For example, visualization in figures 18(*a*) and (*b*) for $Kc = 24$ and 54 respectively shows that the half-cycle wakes are symmetric with respect to the wake centrelines (in both cases these lines are vertical between the cylinders). In each half cycle for such configurations, a small vortex pair from the gap shoots out first, and this is followed by a number of pairs of vortices. Pairing can occur between previous half-cycle vortices with new half-cycle vortices from the outer sides of the cylinders. It is unclear how the gap pairs from one half cycle influence the vortex shedding in a new half cycle. For larger amplitudes than tested here the vortex shedding in each half cycle would approximate to that found for

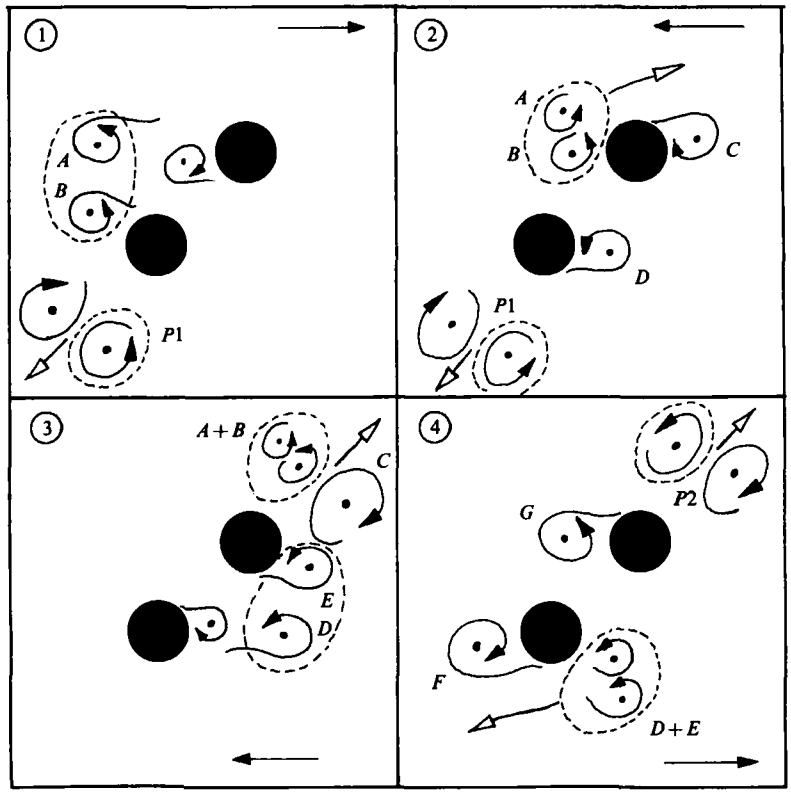

FIGURE 20. Combined 'double-pair' wake for two cylinders at 45° over a large range of Kc ($7 < Kc < 30$) and up to moderate gaps ($g^* < 2.0$). It comprises a large-vortex pair (for example $P1$ or $P2$) convecting away from the cylinders in each half cycle in a direction parallel with the line joining cylinder centres. One feature of the wake is the vortex amalgamation (vortices $A+B$ or $D+E$).

cylinders in a steady stream, where small gaps lead to distinct asymmetry in the wake. For sufficiently small gaps a single wake is formed resembling a limited-length, large-scale Kármán street.

Typical force profiles at $Kc = 28$ for the three orientations of the pair are shown in figure 21. In these diagrams the amplification of the lift signal $Y2$ is 1.9 times that for $Y1$, although for the three orientations in (a), (b) and (c) the scale for $Y1$ remains the same (likewise for $Y2$). Although the timescale is reasonably small, it is possible from this and other force records to determine certain phase relationships between the lift signals. In (a) when two cylinders are side by side the predominance of antiphase lift signals reflects the symmetric half-cycle wakes shown in figure 18. For the small gaps of $g^* = 0.5$ the mean repulsive lift force leads to large repulsive peaks, similar to those found at smaller amplitudes in figure 17 (a).

(ii) *Two cylinders at* 45°. From the present visualization and measurements no predominant shedding pattern seemed to emerge for $Kc > 15$ at larger spacings than $g^* = 2.0$, although for smaller gaps a potentially important 'double-pair' wake is observed for a large range of amplitudes $7 < Kc < 30$. (Below $Kc = 15$ this wake forms when $g^* < 1.0$). The double-pair wake develops out of the combined wakes of the two

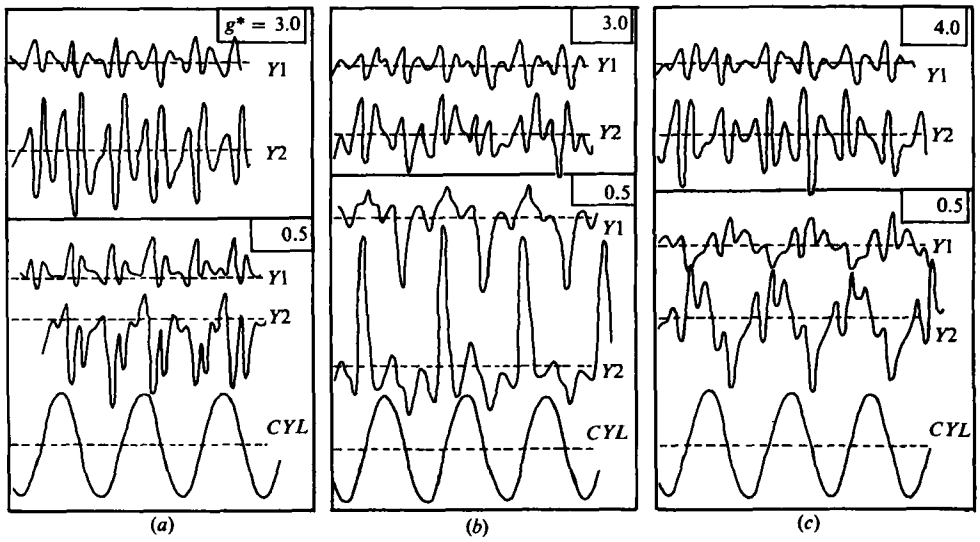

FIGURE 21. Force traces on each cylinder for $Kc = 28$. In (*a*) the cylinders are side by side, in (*b*) they are at 45° and in (*c*) the cylinders are in-line with the oscillation direction. The force profiles (*Y*1, *Y*2) are referred to in the text. Horizontal dashed lines indicate zero levels.

cylinders from a process of pairing and amalgamation of two vortices of the same sign in each half cycle, shown in figure 20. The vortices are observed from a reference frame which travels with the cylinders. In (1), with the cylinders moving to the right, the two vortices A and B are shed in close proximity and pair up in (2) as the flow reverses, to form a large vortex. This amalgamation of vortices (A and B) passes to the right over the upper cylinder in (2) and (3) causing a large vortex C to grow. At the end of this half cycle in (3) the vortex C has paired up with the amalgamated vortices ($A+B$), and convects rapidly away parallel to the line joining the cylinder centres. This vortex pair marked $P2$ in (4) is larger than that associated with one cylinder alone, and it is similar to a pair marked $P1$ formed a half cycle earlier and which is convecting away in the opposite direction. Finally in (4), the pairing of vortex F with the amalgamated vortices ($D+E$) will form a pair similar to $P2$, and so the process continues.

Due to the natural bias of the wake vortex pairs, this wake pattern is particularly repeatable. It also causes very large lift-force peaks for each cylinder in alternate cycles and a mean repulsive lift similar to that found for the side-by-side arrangement. Both of these features are indicated by the force traces in figure 21 (*b*) when $g^* = 0.5$. The peaks are caused by the rapid growth and shedding of a large vortex to complete a vortex pair, and this occurs for each cylinder when it is downstream of the other cylinder. It is possible that this wake pattern may also be found for other orientations in the region of 45° not investigated here.

(iii) *Two cylinders in-line.* In the transverse-street regime the vortex shedding synchronized in-phase with great repeatability when two cylinders were arranged in-line. In the range $15 < Kc < 24$, a double-pair wake for each cylinder tends to form in-phase between the cylinders for $g^* = 2.0$–4.0 but with less repeatability. As relative flow amplitudes are increased further, each half-cycle wake becomes a limited-length Kármán street, as though shed from a single cylinder. For very small gaps the main

wake forms in the rear of the downstream cylinder, otherwise the vortex wake of the upstream cylinder flows round the sides of the downstream cylinder, forming the basis of the downstream wake in each half cycle. In figure 19 the flow visualization is fixed with respect to the cylinders, with the cylinders translating from left to right in (*a*) and near the end of a half cycle in (*b*). The configuration of alternate vortices behind the upstream cylinder in both photographs is similar to the wake which would occur if the downstream cylinder were not present. The magnitude of the lift-force fluctuations in figure 21(*c*) when $g^* = 4.0$ and at $Kc = 24$ are similar to those found for isolated cylinders although, for smaller gaps of $g^* = 0.5$, the lift-force peaks are increased.

4. Force coefficients

4.1. *Force coefficients for a single cylinder*

Root-mean-square coefficients have been evaluated for the isolated cylinder from the U-tube. Values of the 'Morison' coefficients C_m and C_D have also been found (Williamson 1982) and these follow the variation trends found by others, for example Graham (1980). The 'Morison' coefficients are rather sensitive to small phase changes in the in-line-force maxima and such changes are prevalent especially in the transverse-street regime. Another problem with Morison's equation (1) is that it assumes symmetry of the force profile, which is not always a good assumption, as shown clearly from the force trace of figure 6(*c*) for the single-pair wake.

The r.m.s. in-line force coefficients ($C_{\mathrm{F_{rms}}}$) plotted in figure 22(*a*) are relatively insensitive to force-maxima positions as was demonstrated by Maull & Milliner (1978). The r.m.s. force (which includes the pressure-gradient component) is normalized by $(\rho D^3 l/2T^2)$, where l is the cylinder length, and becomes small when Kc is small. An expression for $(C_{\mathrm{F_{rms}}})^2$ derived from (1) contains two terms, one proportional to Kc^2, the other to Kc^4. The coefficients for these powers of Kc are evaluated by finding a straight-line fit to the present data when it is plotted as $(C_{\mathrm{F_{rms}}}/Kc)^2$ versus Kc^2. A surprisingly good representation of the data (the full curve in figure 22*a*) is evaluated as

$$C_{\mathrm{F_{rms}}} = [160Kc^2 + 0.69Kc^4]^{\frac{1}{2}}. \tag{3}$$

The lift force is due solely to the asymmetric vortex growth and motions, and values of lift coefficient ($C_{\mathrm{L_{rms}}}$) in figure 22(*b*) show a reasonable amount of scatter. Such scatter may be caused by average values of $C_{\mathrm{L_{rms}}}$ evaluated over a number of cycles when the vortex shedding intermittently changes mode (for example a transverse street may change from one side of the cylinder to the other). In between modes the lift force shows a random low-amplitude oscillation which has been recorded in both the U-tube and the oscillating cylinder tank. It has been suggested by Bearman *et al.* (1981) that during such times the small-amplitude random profiles are caused by out-of-phase shedding along the cylinder length. Some results from Williamson (1982) have demonstrated, with the use of thin longitudinal fins, how the shedding may be actively encouraged to be out of phase along the cylinder length. Under such conditions, the lift-force profile continually shows the random low-amplitude profile that is found intermittently for a cylinder without fins. This supports the suggestion that the intermittent random lift profiles are indeed caused by out-of-phase vortex shedding.

The three peaks in $C_{\mathrm{L_{rms}}}$ at $Kc \simeq 11$, 18, 26 probably reflect an increase in the repeatability of the shedding patterns. Each peak corresponds with a certain pattern

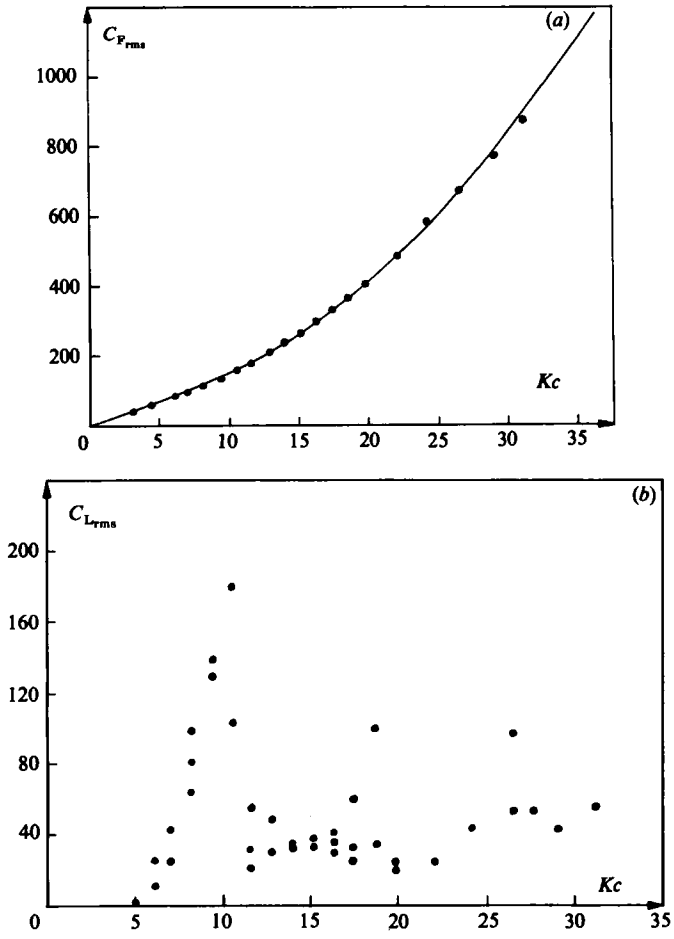

FIGURE 22. (*a*) In-line force r.m.s. coefficients for a range of amplitudes (or Kc). Taken from the U-tube for $\beta = 730$. The points lie closely along a curve given by $C_{F_{rms}} = [160Kc + 0.69Kc^4]^{\frac{1}{4}}$. (*b*) Lift force r.m.s. coefficients for a range of Kc. Taken from the U-tube at $\beta = 730$.

of shedding; in this case the single-pair, double-pair and three-pairs wakes respectively. Similar peaks have been found elsewhere for a coefficient of maximum lift (Bearman *et al.* 1981; Ikeda & Yamamoto 1981). The shedding patterns are probably most repeatable when, at the end of a half cycle, there is a certain configuration of vortices close to the cylinder. Such a configuration close to the cylinder may repeat itself for specific steps of flow amplitude. If we assume that the longitudinal spacing a between vortices of the same sign in steady flow ($a/D \simeq 4.3$, Kármán & Rubach 1912), may be applied approximately to oscillatory flow, then we can estimate the interval of Kc between the most repeatable shedding configurations. A new shedding pattern will emerge every time the flow amplitude increases in steps of $2.15D$, or every time Kc increases by 6.8. This is approximately the interval of Kc found by Ikeda & Yamamoto over which the fundamental vortex frequency increases in steps of one (intervals of 7.5 up to $Kc \simeq 70$) and it is roughly the interval between the present lift-force peaks. It seems that the distance the cylinder needs to travel through a fluid per shed vortex is roughly the same for both steady motion and oscillatory motion, even though in the latter case the acceleration of the cylinder is continually changing.

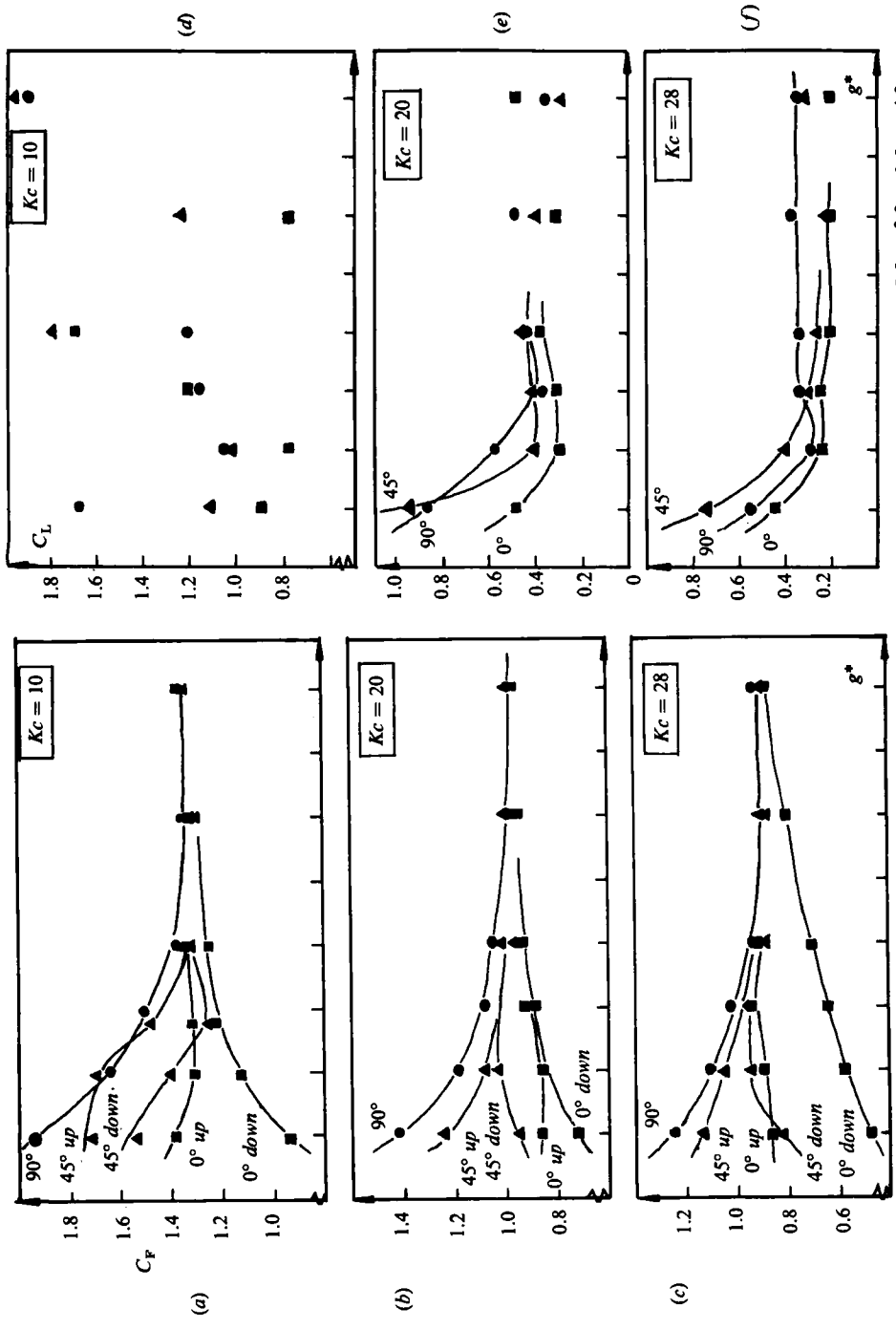

FIGURE 23. Root-mean-square lift and in-line force coefficients for varying gaps and orientations. Each graph corresponds with a particular oscillation amplitude or Kc value. For the in-line force in (*a*)–(*c*) the 'up' and 'down' correspond with the half cycle when the cylinder which is measuring force is upstream and downstream respectively of the other cylinder. The lift coefficients refer to r.m.s. values over complete cycles of oscillation. ●, side by side; ▲, 45° case; ■, in-line.

4.2. *Force coefficients for a pair of cylinders*

In-line and lift forces for the cylinder pair have been measured in the oscillating-cylinder tank. The data has been arranged so that within each graph the oscillation amplitude is a constant, and the orientations and spacing are varied to find their influence on the coefficients. For brevity, only three values of amplitude or Kc are included here ($Kc = 10$, 20, 28), although other amplitudes have been investigated in Williamson (1982). The in-line coefficients are found for upstream and downstream half cycles and the lift coefficients are averaged over the whole cycles and both are normalized by $(\frac{1}{2}\rho U_m^2 Dl)$.

The present in-line forces are measured from the tank and therefore the pressure-gradient component is omitted. However, the variation trends of the in-line force coefficients below should be similar to those in an oscillating flow because, at a constant amplitude in each graph, the pressure-gradient force will have the same cyclic variation whatever the orientation or spacing.

Some of the variation trends of the force coefficients are shown in figure 23 and correspond with certain of the flow patterns described in §3.2. The curves in (*a*), (*b*) and (*c*) represent results for amplitudes of $Kc = 10$, 20 and 28 respectively. For the side-by-side case (90°) the in-line force is markedly increased as the gaps are reduced over the whole range of Kc tested, and corresponds with the antiphase vortex shedding and symmetric wakes, case (i) of §3.2.2). When the cylinders are at 45° and in-line (0°) the upstream in-line force is greater than the downstream force due to a shielding effect of the downstream cylinder by the one upstream. The large increase in the in-line force at 45° for reduced gaps may be associated with the formation of the double-pair combined wake, case (ii) of §3.2.2.

The lift-force coefficients in (*d*), (*e*) and (*f*) also correspond with $Kc = 10$, 20 and 28. It is difficult to draw curves through the data in (*d*) at $Kc = 10$ because there is a large amount of scatter (associated with the large amount of lift-force variation in the region of $Kc = 10$ for a single cylinder in figure 22*b*). However, the lift force generally increases as gaps are reduced for all three orientations. For the 45° case, the high lift at small or moderate gaps is associated with the double-pair wake, which causes large peaks and a mean repulsive lift between the cylinders (shown in §3.2.2). For a side-by-side arrangement, the increase in lift as gaps are reduced is associated with the symmetric wake described above. For the in-line case, the increase in lift is associated with large lift fluctuations on a cylinder when it is in the wake of an upstream cylinder in one of the half cycles.

The present lift-force increase for the 45° case associated with the double-pair combined wake seems in contrast to the results of Sarpkaya who found no lift increase (for his 30° orientation) for gaps below $Kc = 40$. The increase of lift when the cylinders are side by side is also in contrast to his results, which were outlined in §1.

An overall view of how the in-line force varies with flow and geometrical conditions may be found by evaluating values of $C_{\mathrm{F_{rms}}}$ (in this case averaged over full cycles). The similarity in the variation of $C_{\mathrm{F_{rms}}}$ for the whole range of Kc prompted a plot of all the data (for 6 values of Kc) in terms of interference coefficients, in figure 24. The interference coefficient is defined as

$$C_{\mathrm{F_{int}}} = \frac{C_{\mathrm{F_{rms}}}}{C_{\mathrm{F_{rms}}}(\infty)}$$

where $C_{\mathrm{F_{rms}}}(\infty)$ is the isolated cylinder value of $C_{\mathrm{F_{rms}}}$. An approximate single curve is drawn through the points in the side-by-side case and the 45° case, although this

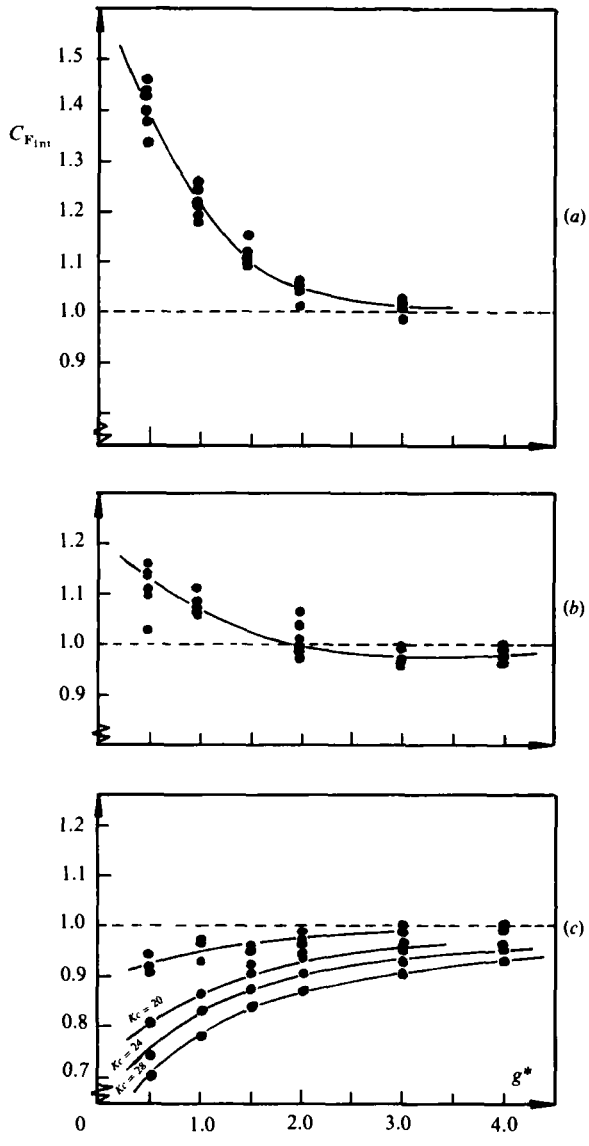

FIGURE 24. In-line interference coefficients for varying gaps. In (*a*) the cylinders are side by side, in (*b*) they are at 45° and in (*c*) the cylinders are in-line with the oscillations. In each graph for each value of g^* the interference coefficients for six values of Kc are plotted (Kc = 10, 13, 16, 20, 24, 28).

is not possible for the in-line case. These graphs show concisely the major effect on total in-line force of varying the cylinder-pair geometry over the whole range of Kc. Clearly the side-by-side case suffers the greatest increase of in-line force with $C_{F_{int}} \simeq 1.5$ for the smallest spacings. The 45° case shows a moderate increase in drag when $g^* < 1.5$. On the other hand, for the in-line case in (*c*) the interference coefficient decreases as gaps are reduced and also as Kc is increased, down to a value of $C_{F_{int}} \approx 0.7$ for $Kc = 28$.

The case of the cylinder pair is the simplest multiple cylinder arrangement. Bushnell suggested, on the basis of force measurements for cylinder groups, that the

two-cylinder case could be used as a model for arrangements involving more cylinders. The type of vortex-shedding synchronization found in the present paper for two cylinders, occurs similarly in a group of four cylinders in a square array, and four cylinders in a row in Williamson (1982). Further investigations of vortex-shedding synchronization and the associated effects on the induced forces may be profitable for larger cylinder arrays, and for higher flow amplitudes.

5. Conclusions

In this paper an isolated cylinder and a pair of cylinders are oscillated in a water tank and, by visualizing the flow simultaneously with the measurement of forces, some of the vortex motions are related to the cylinder forces. Several repeatable patterns of vortex shedding around a single cylinder are directly related to certain regular force fluctuations. These force oscillations may be significant when considering the fatigue life for cylindrical members of a structure in oscillatory flow. In each flow regime the fundamental lift-force frequency is a multiple of the cylinder or flow-oscillation frequency, and this is caused by a specific number of large vortices being shed in each half cycle.

The detailed flow visualization shown in the present paper is taken from an oscillating cylinder rig which allows visualization of the vortex motions in a framework fixed with respect to the undisturbed fluid. Such a framework is in general more effective than one fixed with respect to the cylinder since it allows vortices to be observed without the masking effect of a superposed stream velocity.

The process of vortex pairing between vortices of a previous and present half cycle is fundamental to all the observed vortex patterns, and provides continuity for such patterns. When the vortex wakes are reasonably repeatable, both the lift maximum and r.m.s. values can become comparable to or even exceed those values for the in-line force.

When pairs of cylinders are oscillated in the tank, the flow patterns identified for an isolated cylinder can be modified due to hydrodynamic interference, and therefore produce changes in the cylinder forces. By measuring the lift and in-line forces on both of the cylinders at the same time it is found that not only the vortex shedding but also the induced forces can synchronize in-phase or in antiphase between the cylinders. In-phase synchronization in a complete cylinder array could cause large total lift-force oscillations comparable to the total in-line force, and of a higher frequency. Such an interference effect has not previously been considered.

Under certain conditions the wake from each of the two cylinders can amalgamate forming a large-scale wake, for example the combined double-pair wake observed when two cylinders are at 45° orientation to the direction of oscillation. This vortex pattern in particular is significant in that it induces highly repeatable lift fluctuations with a peak force in excess of three times that found for an isolated cylinder. For each of the three orientations of the present paper (side by side, 45° and in-line with the oscillations) measurements of the r.m.s. forces indicates an increase of both lift and in-line forces as the cylinder spacings are reduced. The only exception is the in-line force for cylinders arranged in-line. The causes of these force magnifications are related to certain vortex motions and their associated fluctuating forces.

A characteristic of the practical case of wave-induced flows around cylinders is the spanwise variation of fluid oscillation amplitudes. Future experimental work will investigate how the vortex patterns described in the present paper for a single cylinder are influenced by a spanwise variation of flow amplitudes. Such work will

include the possibility of forming various different flow patterns simultaneously along the cylinder length. Finally, in the case of cylinder groups it may be important to investigate further the possibilities of vortex-shedding synchronization around cylinders in two-dimensional oscillatory flows and around cylinders in waves. Such investigations could include cylinder arrays which are representative of those found in practice, for example the groups of riser tubes employed beneath offshore platforms.

The author gratefully acknowledges the financial support of the Science and Engineering Research Council C.A.S.E. Award between the University of Cambridge and the National Maritime Institute during the period 1978–81, and the National Maritime Institute during the year 1981–82. The author thanks in particular his academic supervisor, Professor J. E. Ffowcs Williams.

REFERENCES

BEARMAN, P. W., GRAHAM, J. M. R., NAYLOR, P. & OBASAJU, E. 1981 The role of vortices in oscillatory flow about bluff cylinders. *Intl Symp. Hydrodynamics in Ocean Engineering, Norw. Inst. Tech.* pp. 621–626.

BEARMAN, P. W., GRAHAM, J. M. R. & SINGH, S. 1979 Forces on cylinders in harmonically oscillating flow. In *Mechanics of Wave Induced Forces on Cylinders* (ed T. L. Shaw).

BUSHNELL, M. J. 1977 Forces on cylinder arrays in oscillating flow. *OTC Paper* 2903, *Houston, Texas.*

CHAKRABARTI, S. K. 1981 Hydrodynamic coefficients for a vertical tube in an array. *Appl. Ocean Res.* **3**, 2–12.

CHAKRABARTI, S. K. 1982 Transverse forces on vertical tube array in waves. *J. Water, Pt. Coastal Div. ASCE WW1*, **108**.

GRAHAM, J. M. R. 1980 The forces on sharp-edged cylinders in oscillatory flow at low Keulegan–Carpenter numbers. *J. Fluid Mech.* **97**, 331–346.

IKEDA, S. & YAMAMOTO, Y. 1981 Lift force on cylinders in oscillatory flows. *Rep. Dept Found. Engng & Const. Engng, Saitama Univ.* **10**, 1–16.

KARMAN, T. & RUBACH, H. 1912 'Über den Mechanismus des Flüssigkeits- und Luftwiderstandes', *Phys. Zeitschrift* **13**, 49–59.

KEULEGAN, G. H. & CARPENTER, L. H. 1958 Forces on cylinders and plates in an oscillating fluid. *J. Res. Nat. Bur. Stand.* **60**.

LAIRD, A. & WARREN, R. 1963 Groups of vertical cylinders oscillating in water. *J. Engng Mech. Div., ASCE, EM1*, pp. 25–35.

LIGHTHILL, M. J. 1979 Waves and hydrodynamic loading. *BOSS Conf., Imperial College, London*, pp. 1–38.

MAULL, D. J. & MILLINER, M. G. 1978 Sinusoidal flow past a circular cylinder, *Coast Engng* **2**, 149–168.

MORRISON, J. R., O'BRIEN, M. P., JOHNSON, J. W. & SCHAAF, S. A. 1950 The forces exerted by surface waves on piles. *J. Petrol. Tech. Am. Inst. Mining Engng* **189**, 149.

SARPKAYA, T. 1976 In-line and transverse forces on smooth and sand-roughened cylinders in oscillatory flow at high Reynolds numbers. *Naval Postgraduate School, Monterey, Calif.*, NP5-69 Sh76062.

SARPKAYA, T. 1980 Hydrodynamic interference of two cylinders in harmonic flow. *OTC Paper* 3775, *Houston, Texas.*

WILLIAMSON, C. H. K. 1982 Cylinders in unsteady flow. PhD thesis, Dept. of Engineering, University of Cambridge.

ZDRAVKOVICH, M. 1977 Interference between two circular cylinders; series of unexpected discontinuities. *J. Ind. Aerod.* **2**, 255–270.